الجمهورية الجزائرية الديمقراطية الشعبية

Republic Algeria Democratic and Popular

وزارة التعليم العالي والبحث العلمي

Ministry of Higher Education and Scientific Research

University of Blida 1

Institute of Aeronautics and Aerospace Studies

End of studies project in order to obtain a Master's degree in Aeronautics

Specialty : Spatial Telecommunications

Theme:

Design and Simulation of Two Elements Array Antenna for Satellite Communications

Realized by:

- **KHALFAOUI** Mohamed Amine.
- **HADJERSI** Yasser.

Under the supervision of:

- **Dr. MOUFFOK** Lila.

2020/2021

Dedication

This thesis is dedicated to:

“My family, the symbol of love and giving, my friends who encouraged and supported me, and for whoever was the reason I was able to make it this far.”

- KHALFAOUI Mohamed Amine.

“Mom and Dad who always pick me up on time and encouraged me to go on every adventure, specially this one, my grandmother, who never stopped pushing me in countless ways, my beloved brothers and my dear friends.”

- HADJERSI Yasser.

Acknowledgment

In the Name of Allah, the Most Merciful, the Most Compassionate all praise be to Allah, the Lord of the worlds; and prayers and peace be upon Mohamed His servant and messenger. First and foremost, we must acknowledge my limitless thanks to Allah, the Ever-Magnificent; the Ever-Thankful, for His helps and bless.

We would like to express our special appreciation and thanks to our advisor Dr. MOUFFOK Lila for encouraging our research and for allowing us to take a step forward. We would like to thank the faculty and administration of institute of Aeronautics and Space Studies (IAES), for the wealth and quality of their teaching and making great efforts to ensure to their students. A special thanks to our family. Words cannot express how grateful we are to our mothers and our fathers for all of the sacrifices that they've made on our behalf. Your prayer for us was what sustained us thus far, without forgetting to thank our brothers and sisters.

Finally, we would like express my gratitude to all the people who helped me by providing their valuable assistance and time.

Abstract

The thesis proposes reconfigurable antenna designs with combined frequency and pattern reconfigurable characteristics. The main focus is first to examine the exploitation of a single-element antenna structure. An optimization procedure including a study of relevant design parameters is also presented. The structure has a controllable active component that allows the antenna to be tuned to different operating frequencies which is the Varactor diode. Next, the thesis focuses on the manipulation of near-resonant current distributions in a two-element array antenna based on the same operation principle, as well as the optimization of their feeding through T-junction power dividers. The core contribution for the two-element array and the single-element antenna is that they combine frequency-reconfigurability with effective beam scanning.

Résumé

La thèse propose des conceptions d'antennes reconfigurables avec des caractéristiques reconfigurables combinées de fréquence et de diagramme. L'objectif principal est d'abord d'examiner l'exploitation d'une structure d'antenne à un seul élément. Une procédure d'optimisation comprenant une étude des paramètres de conception pertinents est également présentée. La structure a un composant actif contrôlable qui permet à l'antenne d'être réglée sur différentes fréquences de fonctionnement qui est la diode Varactor. Ensuite, la thèse se concentre sur la manipulation des distributions de courant quasi-résonnant dans une antenne réseau à deux éléments basée sur le même principe de fonctionnement, ainsi que sur l'optimisation de leur alimentation par des diviseurs de puissance à jonction en T. La contribution principale du réseau à deux éléments et de l'antenne à un seul élément est qu'ils combinent la reconfigurabilité de la fréquence avec un balayage efficace du faisceau.

ملخص

تقترح المذكرة تصاميم هوائيات قابلة لإعادة التشكيل مع الخصائص المشتركة للتردد والنمط القابلة لإعادة التشكيل. وأول ما يركز هو دراسة استغلال هيكل هوائي أحادي العنصر. كما يتم تقديم إجراء التحسين بما في ذلك دراسة معلمات التصميم ذات الصلة. يحتوي الهيكل على مكون نشط يمكن التحكم فيه يسمح بضبط الهوائي على ترددات تشغيل مختلفة وهو الصمام الثنائي Varactor. بعد ذلك، تركز الأطروحة على التلاعب بالتوزيعات الحالية شبه الرنانة في هوائي صفيف من عنصرين استنادا إلى نفس مبدأ التشغيل، بالإضافة إلى تحسين تغذيتها من خلال فواصل الطاقة على شكل T-junction. والمساهمة الأساسية للصفيف ذو العنصرين والهوائي أحادي العنصر هي أنهما يجمعان بين إمكانية إعادة تشكيل التردد والمسح الضوئي الفعال للشعاع.

Summary

Figures List

Tables List

Abbreviations

PCB: Printed Circuit Board.

MPA: Microstrip Patch Antenna.

dB: Decibels.

RFID: Radio Frequency Identification.

WiMax: Worldwide Interoperability for Microwave Access.

WBAN: Wireless Body Area Network.

IEEE: Institute of Electrical and Electronics Engineers.

RF: Radio-Frequency.

RF MEMS: Radio-Frequency MicroElectroMechanical System.

DC: Direct Current.

VSAT: Very Small Aperture Terminal.

ISS: International Space Station.

NASA: National Aeronautics and Space Administration.

BSS: Broadcasting Satellite Service.

CP: Circular Polarized.

RHCP: Right Hand Circular Polarized.

LHCP: Left Hand Circular Polarized.

EM: Electromagnetic.

Introduction

The fundamentals of antenna theory and design have been introduced since 1888, researches in the telecommunication technologies haven't stopped since then, especially during the few past years where a new era in antenna technology is currently underway due to the ubiquity of wireless connectivity Over the past decades, numerous approaches have been implemented to achieve sophisticated properties of reconfigurable antennas by controlling the surface current distribution or modifying the electrical structure of the antenna without changing the physical geometry. A lot of applications have been made in this field within the frequency of 2.4 GHz.

Our objective in this thesis is to achieve adaptive variations of antenna characteristics, including operating frequency, gain, impedance matching and radiation patterns in the framework of reconfigurable designs within the Ku-band frequency. We are going to present an in-depth understanding of the fundamental parameter characteristics that are important to achieve reliable designs of antennas with predictable reconfiguration properties.

This thesis will be divided into 3 main chapters, each one of them is virtually self-contained and will deal with a different topic.

The first chapter provides a brief explanation of the context of microstrip antennas and microwave systems. It also gives some general introductions and information about some telecommunication related terms that will be used during our work in this thesis.

Chapter 2 describes in detail the possible mechanisms and techniques commonly used to achieve reconfiguration of antennas in terms of frequency, radiation pattern, polarization or compound properties. It also includes some of the examples that were recently published works illustrating theoretical applications, potential and constraints of reconfigurable antenna design approach.

The 3rd chapter involves the analysis, design and measurement of reconfigurable microstrip antenna designs for beam scanning purposes, according to array antenna operating principles in the Ku-band. It also introduces dual and single-element microstrip antenna configurations with integrated stub-loaded varactors as a tuning mechanism to achieve a reconfiguration of operating frequency concurrently to a continuous scanning of the radiation patterns.

Chapter 1

General Information on Microstrip Antennas

In telecommunication, a microstrip antenna (also known as a printed antenna) usually means an antenna fabricated using photolithographic techniques on a printed circuit board (PCB). It is a kind of internal antenna. They are mostly used at microwave frequencies. This chapter presents some of the general information that needs to be known before checking out some of its implementations and uses, and how it is going to be reconfigured.

1.1 Introduction

In radio engineering, an antenna or aerial is the interface between radio waves propagating through space and electric currents moving in metal conductors, used with a transmitter or receiver. In transmission, a radio transmitter supplies an electric current to the antenna's terminals, and the antenna radiates the energy from the current as electromagnetic waves (radio waves). In reception, an antenna intercepts some of the power of a radio wave in order to produce an electric current at its terminals, that is applied to a receiver to be amplified. Antennas are essential components of all radio equipment.

1.2 Microstrip Patch Antenna

A microstrip patch antenna (MPA) consists of a conducting patch of any planar or nonplanar geometry on one side of a dielectric substrate with a ground plane on other side. It is a popular printed resonant antenna for narrow-band microwave wireless links that require semi-hemispherical coverage. Due to its planar configuration and ease of integration with microstrip technology, the microstrip patch antenna has been heavily studied and is often used as elements for an array. A large number of microstrip patch antennas have been studied to date [1]. An exhaustive list of the geometries along with their salient features is available. The rectangular and circular patches are the basic and most commonly used microstrip antennas. These patches are used for the simplest and the most demanding applications. Rectangular geometries are separable in nature and their analysis is also simple. The circular patch antenna has the advantage of their radiation pattern being symmetric. A rectangular microstrip patch antenna in its simplest form is shown in Figure 1.1, where W is its width and L is its length, and h is its dielectric substrate.

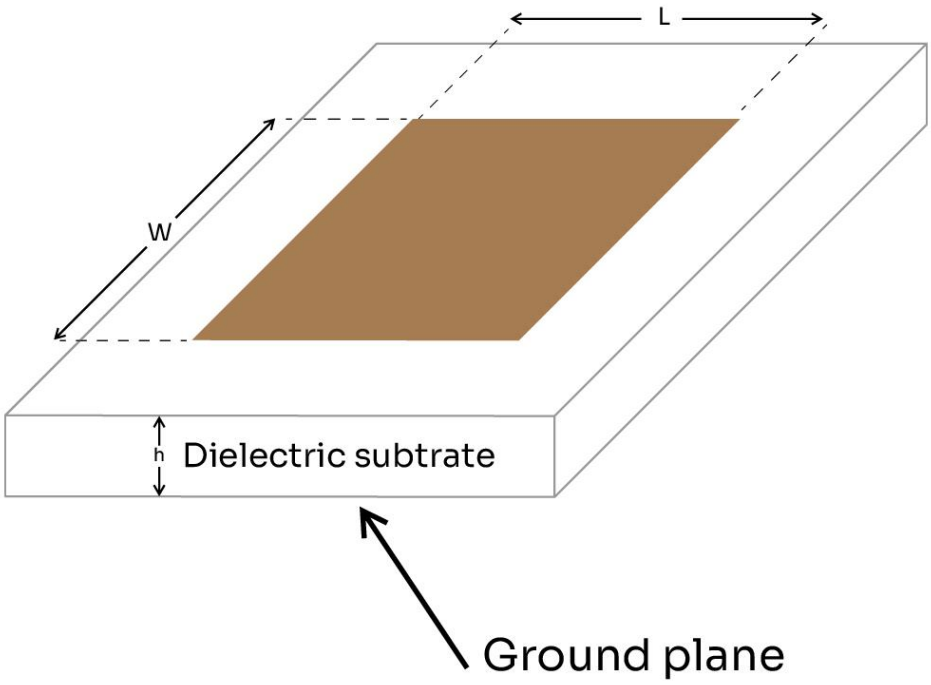

Figure 1.1: Structure of a rectangular Microstrip Patch Antenna.

In the wide range of antenna models there are different structures of Microstrip antennas, but on the whole, we have four basic parts in the antenna, they are:

- The patch
- Dielectric Substrate
- Ground Plane
- Feed Line

1.3 Feeding Techniques

A feedline is used to excite by direct or indirect contact. There are many different techniques of feeding and four most popular techniques are coaxial probe feed, microstrip line, aperture coupling and proximity coupling.

Coaxial probe feeding is feeding method in which that the inner conductor of the coaxial is attached to the radiation patch of the antenna while the outer conductor is connected to the ground plane. Advantages of coaxial feeding is easy of fabrication, easy to match, low spurious

radiation and its disadvantages is narrow bandwidth, Difficult to model specially for thick substrate (Figure 1.2).

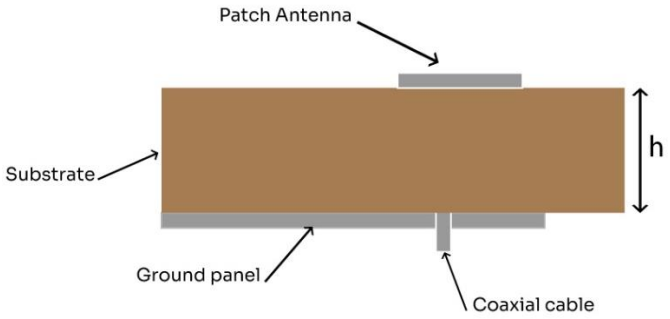

Figure 1.2: Coaxial probe feed patch.

Microstrip line feed is one of the easier methods to fabricate as it is a just conducting strip connecting to the patch and therefore can be consider as extension of patch [2]. It is simple to model and easy to match by controlling the inset position. However, the disadvantage of this method is that as substrate thickness increases, surface wave and spurious feed radiation increases which limit the bandwidth. A rectangular feedline in its simplest form is shown in Figure 1.3.

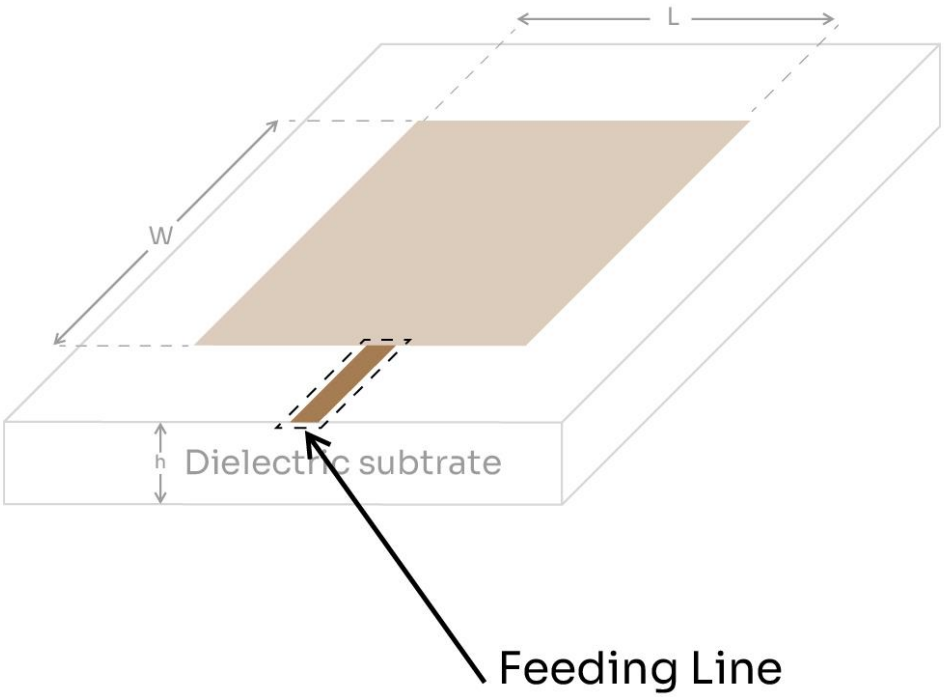

Figure 1.3: A Microstrip Patch Antenna's Feedline.

Aperture coupled feed consist of two different substrates separated by a ground plane. On the bottom side of lower substrate there is a microstrip feed line whose energy is coupled to the patch through a slot on the ground plane separating two substrates. This arrangement allows independent optimization of the feed mechanism and the radiating element. Normally top substrate uses a thick low dielectric constant substrate while for the bottom substrate; it is the high dielectric substrate. The ground plane, which is in the middle, isolates the feed from radiation element and minimizes interference of spurious radiation for pattern formation and polarization purity. Advantages is allowing independent optimization of feed mechanism element, as showed in Figure 1.4 down below:

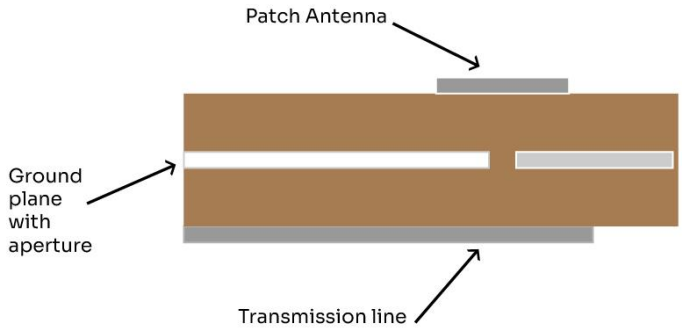

Figure 1.4: *Aperture coupled feed patch antenna.*

Proximity coupling has the largest bandwidth, has low spurious radiation. However, fabrication is difficult. Length of feeding stub and width-to-length ratio of patch is used to control the match. Its coupling mechanism is capacitive in nature (Figure 1.5). The major disadvantage of this feeding technique is that it is difficult to fabricate because of the two dielectric layers that need proper alignment. Also, there is increase in overall thickness of the antenna.

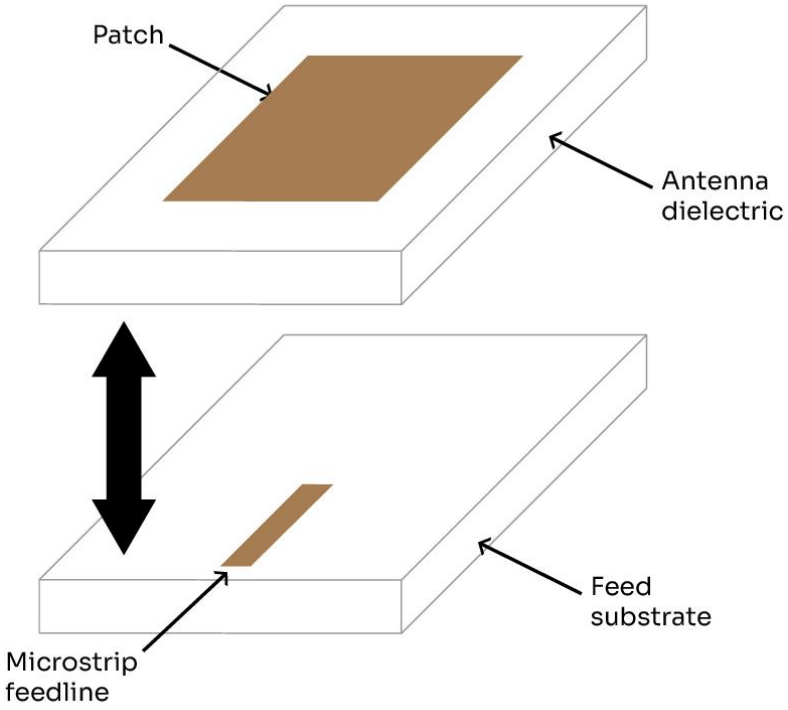

Figure 1.5: *Proximity coupled microstrip patch antenna.*

1.4 Characteristics

Irrespective of the application that an antenna is used in, all the antennas are associated with a few fundamental parameters. These parameters are sometimes also called as Properties of Antenna or Characteristics of Antenna [3]. Certain basic characteristics of antenna are listed below:

- Antenna Radiation Pattern
- Efficiency
- Bandwidth
- Gain
- Directivity
- Reflection coefficient
- Antenna Impedance

1.4.1 Radiation Pattern

The radiation pattern is a graphical depiction of the relative field strength transmitted from or received by the antenna, and shows sidelobes and back lobes. As antennas radiate in space often several curves are necessary to describe the antenna. If the radiation of the antenna is symmetrical about an axis (as is the case in dipole, helical and some parabolic antennas) a unique graph is sufficient [4].

Each antenna has different standards as well as plotting formats. Each format has its own advantages and disadvantages. Radiation pattern of an antenna can be defined as the locus of all points where the emitted power per unit surface is the same. The radiated power per unit surface is proportional to the squared electrical field of the electromagnetic wave. The radiation pattern is the locus of points with the same electrical field. In this representation, the reference is usually the best angle of emission. It is also possible to depict the directive gain of the antenna as a function of the direction. Often the gain is given in decibels (dB).

The graphs can be drawn using cartesian (rectangular) coordinates or a polar plot. This last one is useful to measure the beamwidth, which is, by convention, the angle at the -3 dB points around the max gain. The shape of curves can be very different in cartesian or polar coordinates

and with the choice of the limits of the logarithmic scale. The Figure 1.6 below represents the radiation patterns of a same half-wave antenna in 3 different ways.

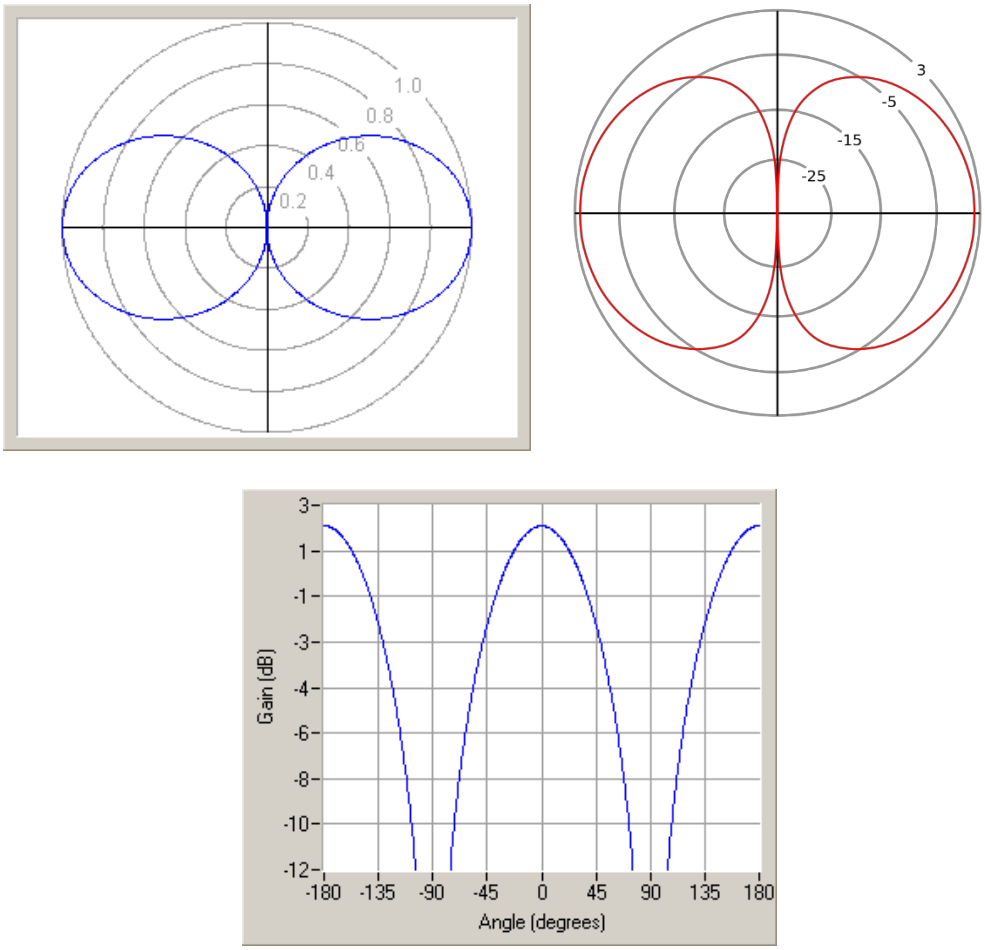

Figure 1.6: Radiation patterns of a same half-wave antenna.

1.4.2 Efficiency

Efficiency is the ratio of power actually radiated by an antenna to the electrical power it receives from a transmitter. It is defined as the ratio of the power that is radiated to the total power used by the antenna; Total power = power radiated + power loss [5].

$$\tilde{n} = \frac{P_r}{P_r + P_l} \qquad (1.1)$$

1.4.3 Bandwidth

Bandwidth is the difference between the upper and lower frequencies in a continuous band of frequencies. It is typically measured in hertz, and depending on context, may specifically refer to passband bandwidth or baseband bandwidth. Passband bandwidth is the difference between the upper and lower cutoff frequencies of, for example, a band-pass filter, a communication channel, or a signal spectrum [6]. Baseband bandwidth applies to a low-pass filter or baseband signal; the bandwidth is equal to its upper cutoff frequency.

To calculate the bandwidth, we use:

$$B = \Delta f = f_H - f_L \tag{1.2}$$

where f_H and f_L are the upper and lower frequency limits respectively of the band in question.

1.4.4 Gain

Gain as a parameter measures the directionality of a given antenna. An antenna with a low gain emits radiation in all directions equally, whereas a high-gain antenna will preferentially radiate in particular directions. Specifically, the Gain or Power gain of an antenna is defined as the ratio of the intensity (power per unit surface) radiated by the antenna in a given direction at an arbitrary distance divided by the intensity radiated at the same distance by a hypothetical isotropic antenna:

$$G = \frac{(\frac{P}{S})_{ant}}{(\frac{P}{S})_{iso}} \tag{1.3}$$

The word "hypothetical" is used because a perfect isotropic antenna cannot be constructed.

Gain is a dimensionless number (without units) and it is a passive phenomenon, power is not added by the antenna, but simply redistributed to provide more radiated power in a certain direction than would be transmitted by an isotropic antenna. If an antenna has a greater than one gain in some directions, it must have a less than one gain in other directions since energy is conserved by the antenna. An antenna designer must take into account the application for the antenna when determining the gain. High-gain antennas have the advantage of longer range

and better signal quality, but must be aimed carefully in a particular direction. Low-gain antennas have shorter range, but the orientation of the antenna is inconsequential.

Realized Gain of an antenna refers to the evaluation of gain of a particular antenna, while taking into account the reflections losses that occurs at the input terminals as well as losses within the structure of the antenna [7].

1.4.5 Directivity

Directivity is a parameter which measures the degree to which the radiation emitted is concentrated in a single direction. It measures the power density the antenna radiates in the direction of its strongest emission, versus the power density radiated by an ideal isotropic radiator (which emits uniformly in all directions) radiating the same total power [8].

An antenna's directivity is a component of its gain; the other component is its (electrical) efficiency. It is the maximal value of its directive gain. Directive gain is represented as $D(\theta,\varphi)$ and compares the radiant intensity (power per unit solid angle) $U(\theta,\varphi)$ that an antenna creates in a particular direction against the average value over all directions:

$$D(\theta,\varphi) = \frac{U(\theta,\varphi)}{P_{tot}/(4\pi)} \tag{1.4}$$

Here θ and φ are the zenith angle and azimuth angle respectively in the standard spherical coordinate angles; $U(\theta,\varphi)$ integrated over a spherical surface. Since there are 4π steradians on the surface of a sphere, the quantity $P_{tot}/(4\pi)$ represents the average power per unit solid angle.

In other words, directive gain is the radiation intensity of an antenna at a particular (θ,φ) coordinate combination divided by what the radiation intensity would have been had the antenna been an isotropic antenna radiating the same amount of total power into space.

In decibels:

$$D_{dBi} = 10.log_{10}(D(\theta,\varphi)) \tag{1.5}$$

1.4.6 Reflection coefficient

In the context of antennas and feeders, the reflection coefficient is defined as the figure that quantifies how much of an electromagnetic wave is reflected by an impedance discontinuity in the transmission medium. The reflection coefficient is equal to the ratio of the amplitude of the reflected wave to the incident wave.

There are many ways in which the reflection coefficient can be calculated.

Using the basic definition of the reflection coefficient, it can be calculated from a knowledge of the incident and reflected voltages, as shown in Figure 1.7 down below.

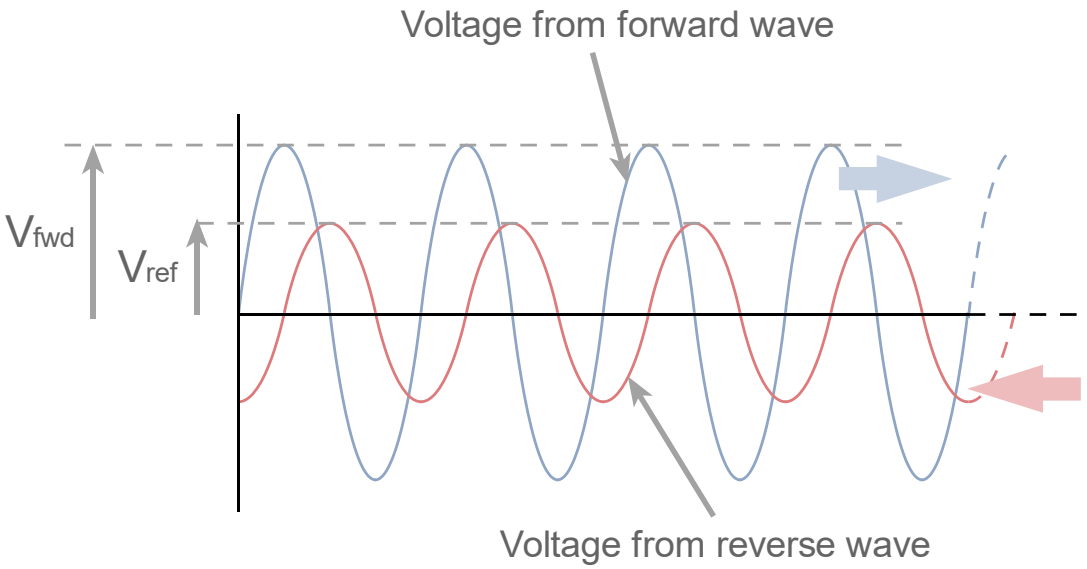

Figure 1.7: *Voltages used for calculating the reflection coefficient.*

$$S_{11} = \Gamma = \frac{V_{ref}}{V_{fwd}} \tag{1.6}$$

Where:

S_{11}, Γ is the reflection coefficient.

V_{ref} is the reflected voltage.

V_{fwd} is the forward voltage.

It is also possible to express the reflection coefficient in terms of the load and line or feeder impedances, as the Figure 1.8 shows:

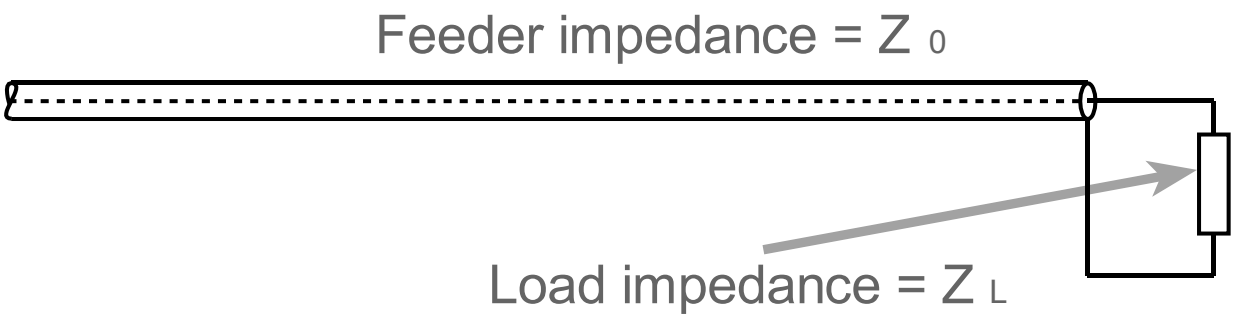

Figure 1.8: *The feeder and load impedance definitions.*

$$S_{11} = \Gamma = \frac{|Z_L - Z_0|}{|Z_L + Z_0|} \qquad (1.7)$$

Where:

Z_L is the load impedance.

Z_0 is the feeder characteristic impedance.

1.4.7 Antenna impedance

Antenna impedance is a measure of the resistance to an electrical signal in an antenna. Many factors have an impact on an antenna's ability to transmit a signal, including the environment that the antenna is in and the design and composition of the antenna. Understanding antenna impedance is important when designing components that connect an antenna to a receiver or transmitter. The ratio of voltage to current, which is equal to antenna impedance, is expressed in [Ω] ohms. The antenna impedance represents the power that is absorbed by the antenna as well as the power that is dispersed by it as it comes into contact with an electromagnetic wave. Different wavelengths of electromagnetic radiation will give the same antenna different impedance values.

1.5 Applications

The Microstrip patch antennas are well known for their performance and their robust design, fabrication and their extent usage. The advantages of this Microstrip patch antenna are to overcome their de-merits such as easy to design, light weight etc., the applications are in the various fields such as in the medical applications, satellites and of course even in the military systems just like in the rockets, aircrafts missiles etc. the usage of the Microstrip antennas are spreading widely in all the fields and areas and now they are booming in the commercial aspects due to their low cost of the substrate material and the fabrication. It is also expected that due to the increasing usage of the patch antennas in the wide range this could take over the usage of the conventional antennas for the maximum applications. Microstrip patch antenna has several applications. Some of these applications are discussed as below:

- **Mobile and satellite communication application:** Mobile communication requires small, low-cost, low profile antennas. Microstrip patch antenna meets all requirements and various types of microstrip antennas have been designed for use in mobile communication systems. In case of satellite communication circularly polarized radiation patterns are required and can be realized using either square or circular patch with one or two feed points.
- **Global Positioning System applications:** Nowadays microstrip patch antennas with substrate having high permittivity sintered material are used for global positioning system. These antennas are circularly polarized, very compact and quite expensive due to its positioning. It is expected that millions of GPS receivers will be used by the general population for land vehicles, aircraft and maritime vessels to find their position accurately.
- **Radio Frequency Identification (RFID):** RFID uses in different areas like mobile communication, logistics, manufacturing, transportation and health care [2]. RFID system generally uses frequencies between 30 Hz and 5.8 GHz depending on its applications. Basically, RFID system is a tag or transponder and a transceiver or reader.

- **Worldwide Interoperability for Microwave Access (WiMax):** The IEEE 802.16 standard is known as WiMax. It can reach up to 48280 meters radius theoretically and data rate 70 Mbps. MPA generates three resonant modes at 2.7, 3.3 and 5.3 GHz and can, therefore, be used in WiMax compliant communication equipment [9].
- **Radar Application:** Radar can be used for detecting moving targets such as people and vehicles. It demands a low profile, light weight antenna subsystem, the microstrip antennas are an ideal choice. The fabrication technology based on photolithography enables the bulk production of microstrip antenna with repeatable performance at a lower cost in a lesser time frame as compared to the conventional antennas.
- **Telemedicine Application:** In telemedicine application antenna is operating at 2.45 GHz. Wearable microstrip antenna is suitable for Wireless Body Area Network (WBAN). The proposed antenna achieved a higher gain and front to back ratio compared to the other antennas, in addition to the semi directional radiation pattern which is preferred over the omni-directional pattern to overcome unnecessary radiation to the user's body and satisfies the requirement for on-body and off-body applications. An antenna having gain of 6.7 dB and a F/B ratio of 11.7 dB and resonates at 2.45GHz is suitable for telemedicine applications.
- **Medicinal applications of patch:** It is found that in the treatment of malignant tumors the microwave energy is said to be the most effective way of inducing hyperthermia. The design of the particular radiator which is to be used for this purpose should possess light weight, easy in handling and to be rugged. Only the patch radiator fulfils these requirements. The initial designs for the Microstrip radiator for inducing hyperthermia was based on the printed dipoles and annular rings which were designed on S-band. And later on, the design was based on the circular microstrip disk at L-band.

1.6 Array Antenna

Microstrip antennas are used in arrays as well as single elements. By using array in communication systems, we enhance the performance of the antenna like increasing gain, directivity scanning the beam of an antenna system, and other functions which are difficult to do with the single element.

1.6.1 Linear Microstrip Arrays

Linear arrays are used for fan-shaped coverage and can also form a building block for planar arrays. Some case examples are provided to illustrate the design procedure. The three main feed methods are shown in Figure 1.9.

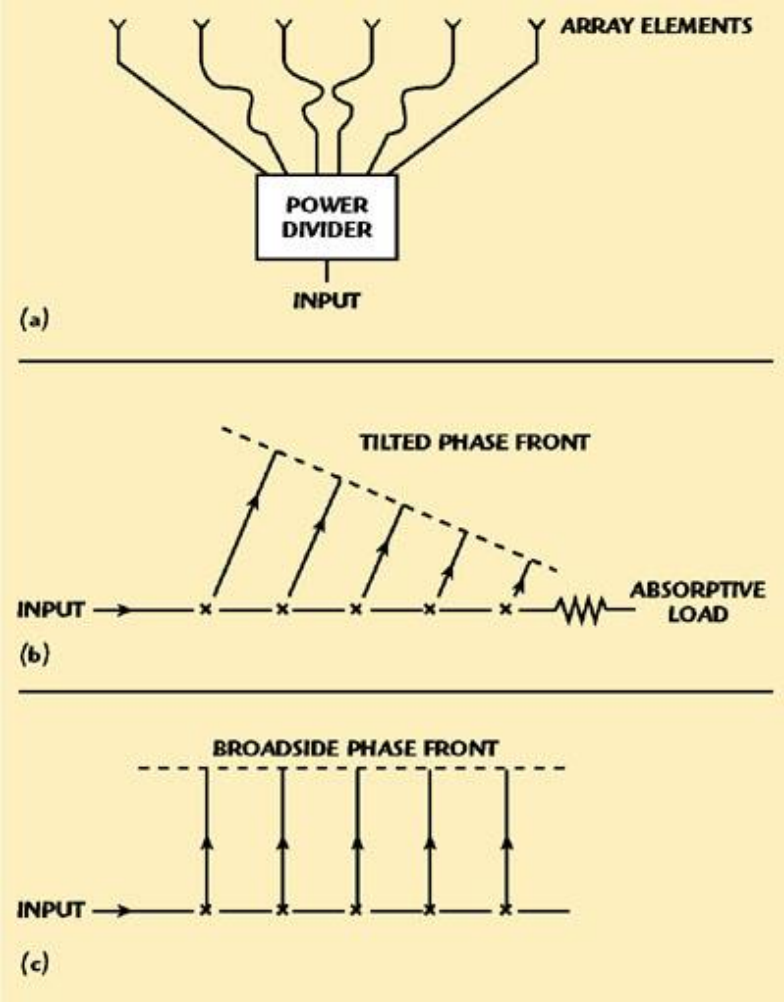

Figure 1.9: *Linear array fields; (a) corporate, (b) travelling wave, (c) resonant feeds.*

First, the corporate feed, which is composed of a power divider with transmission lines to the individual radiators, is examined. Although this method is physically large and expensive, it is also the most broadband. Often the overall bandwidth is limited by the bandwidth of the radiators themselves. Corporate feeds are popular for phased arrays where phase shifters are inserted in the transmission lines to steer the beam direction electrically.

Next, the travelling wave feed is described. Radiators are coupled to a single transmission line and energy decays along the line length. To achieve a symmetrical radiated power distribution the radiator coupling factors are made asymmetrical. An absorptive load captures the remaining energy. It is important that the radiator spacing is not a multiple of half a guide wavelength so that reflections from the radiators have a different phase at the feed input and tend to cancel each other. As a result, the beam is tilted from broadside in a travelling wave antenna. A good input match is generally obtained, but it helps, especially for short arrays using tight radiator coupling factors, to incorporate a matching section at each radiator. The bandwidth is often limited by the permitted beam pointing variation.

Finally, there is the resonant array. Here radiators are deliberately spaced a multiple of half a guide wavelength apart to produce a broadside pointing beam. Some radiator types can be represented by a shunt conductance and others are represented by a series resistance. For the former, the input voltage repeats at each radiator and the input conductance is equal to the sum of the individual radiation conductance (usually made equal to the characteristic admittance of the microstrip line for a good match). In the case of series radiators, the current repeats at each radiator and the input resistance is equal to the sum of the individual radiation resistances. No absorptive load is used in either case and the radiator coupling factors are symmetrical for a symmetrical power distribution at the aperture. The match usually limits the bandwidth.

1.6.2 Planar Microstrip Arrays

Planar microstrip arrays are used to form a pencil beam and array elements can be fed in a variety of ways. One of the ways is shown in Figure 1.10, which consists of patch radiators and a network of microstrip feed lines. The patch feeds are inset to achieve a good match to the feed lines. The feed lines are made of similar length so the beam pointing is broadside to the array at all frequencies. The bandwidth is limited by the patches themselves, which is typically a few percent. Feed lines are rather long, adding to loss mechanisms, and spurious radiation is caused at bends and junctions.

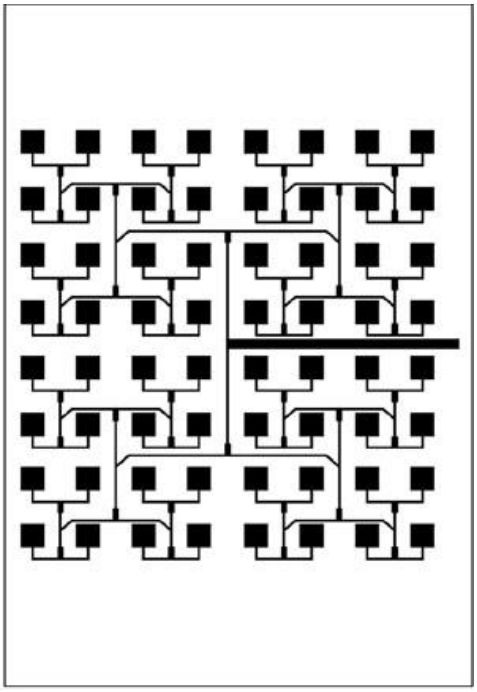

Figure 1.10: Planar array corporate feed network.

Calculating directivity in an antenna array

$$D_{array}(\theta,\varphi) = |AF|^2 \times D(\theta,\varphi) \tag{1.8}$$

Where $D(\theta,\varphi)$ is the directivity of a single element. This single element term is sometimes referred to as the element pattern, and AF is the array factor;

$$AF(\hat{r}) = \sum_{n=1}^{N} a_n \, e^{jk\hat{r}.\vec{r}_n} \tag{1.9}$$

Where a_n are the complex-valued excitation coefficients, and $\hat{r}$ is the direction unit vector.

1.7 Conclusion

A theoretical survey on microstrip patch antenna is presented in this chapter. Lower gain and low power handling capacity can be overcome through an array configuration. Some factors are involved in the selection of feeding technique. Particular microstrip patch antenna can be designed for each application and different merits are compared with conventional microwave antenna.

Chapter 2

Reconfigurable Antennas for Ku band

In this chapter, reconfigurable antennas will be more explained and deeper introduced, it'll presents the different ways that an antenna can be reconfigured with, and the various results achieved by it, also, Ku band and other priorities will be illustrated.

2.1 Introduction

In wireless mobile communication systems applications, microstrip antennas are particularly attractive due to their low profile, light weight, and easy fabrication. Antennas used in complicated systems are required to be multi-frequency and multi-function; such as sweep or change of operation frequency, adaptation of the radiation pattern, polarization etc... For example, to achieve several resonance frequencies using patch antenna technology, a few separate antennas can be designed. Instead, a re-configurable antenna will be more convenient and will occupy less area. Wideband antennas might be better, if can be implemented for the specific application.

2.2 Reconfigurable Antennas in Microwave Systems

With the advancement of new communications, reconfigurable antennas have emerged as promising solution to achieve high performance designs in microwave systems. This has fostered an increasing level of research activities in this field over the past years. This is because the development of reconfigurable antennas provides potentially more effective designs with high flexibility in functionalities that would be almost impossible to achieve in a static implementation. Reconfigurable antennas also could prove to become a necessary solution in industrial applications to extend functionalities beyond the limitations of conventional antenna systems [1].

Generally, the microwave region is physically defined in the electromagnetic spectrum as covering the frequency range in between 500 MHz (1 m wavelength) to 300 GHz (1 mm wavelength), Figure 2.1 situates the microwave frequency region in the electromagnetic spectrum together with the denominations commonly used to describe frequency bands [3].

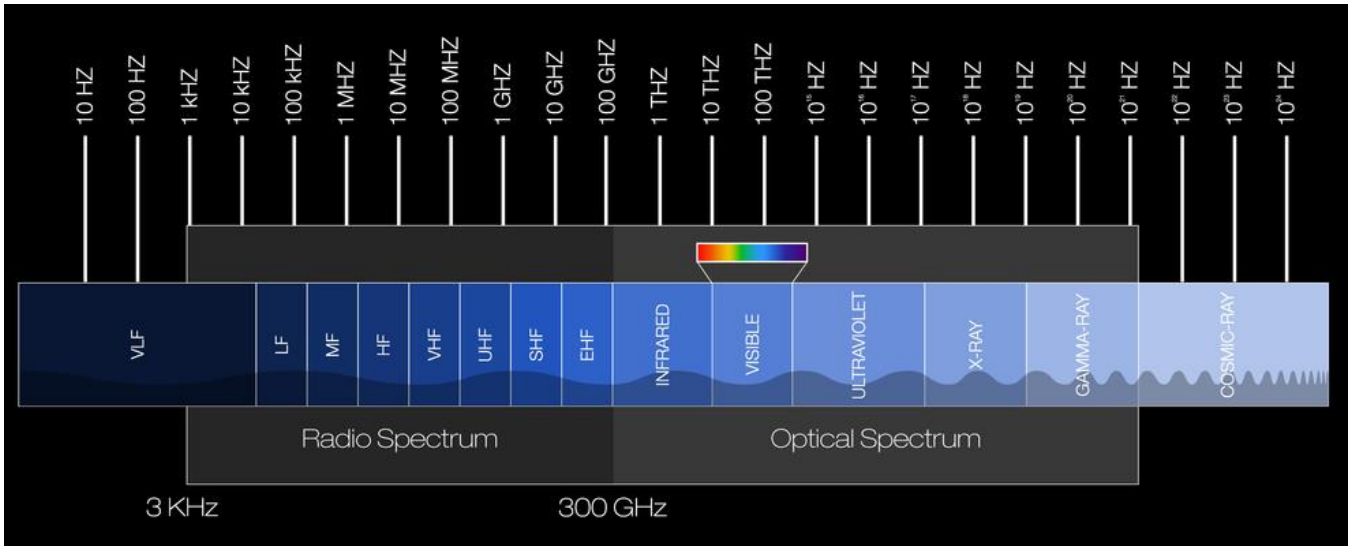

Figure 2.1: A classification of electromagnetic spectrum.

The microwave range possesses some of the most relevant features enabling efficient wireless communications and remote sensing systems. This motivates the development of small antennas to help miniaturization of systems, especially for systems operating at lower frequencies. There are however physical limits to miniaturization, and therefore, the concept of reconfigurable or agile antennas can provide a solution by clustering several functionalities into a single antenna, thus relaxing the space and weight problems associate with multiple antennas configurations.

IEEE Radar Band Designations:

Band	**HF**	**VHF**	**ULF**	**L**	**S**	**C**	**X**	**K**	**Ku**	**Ka**
Frequencies	3-30 **MHz**	30-300 **MHz**	300-1000 **MHz**	1-2 **GHz**	2-4 **GHz**	4-8 **GHz**	8-12 **GHz**	12-18 **GHz**	18-27 **GHz**	27-40 **GHz**
Wavelength	100-10 m	10–1 m	100–30 cm	30-15 cm	15-7.5 **cm**	7.5-3.7 cm	3.7-2.5 cm	2.5-1.6 cm	1.6-1.1 cm	11-7.5 mm

Table 1: IEEE Radar Band Designations.

2.3 Reconfiguration Mechanisms

Figure 2.2 provides a brief overview of various mechanisms and advanced techniques that can be adopted into reconfigurable antenna designs. Every approach has associated practical techniques which should be considered in view of their advantages and disadvantages for the intended application; In this section, the electrical tuning methods will be described in more detail since they are the most relevant today, and they are the subject of this thesis. Electrical reconfigurability techniques include different switching modalities enabled by Radio Frequency MicroElectroMechanical Systems (RF MEMS) switches, PIN diodes and varactors.

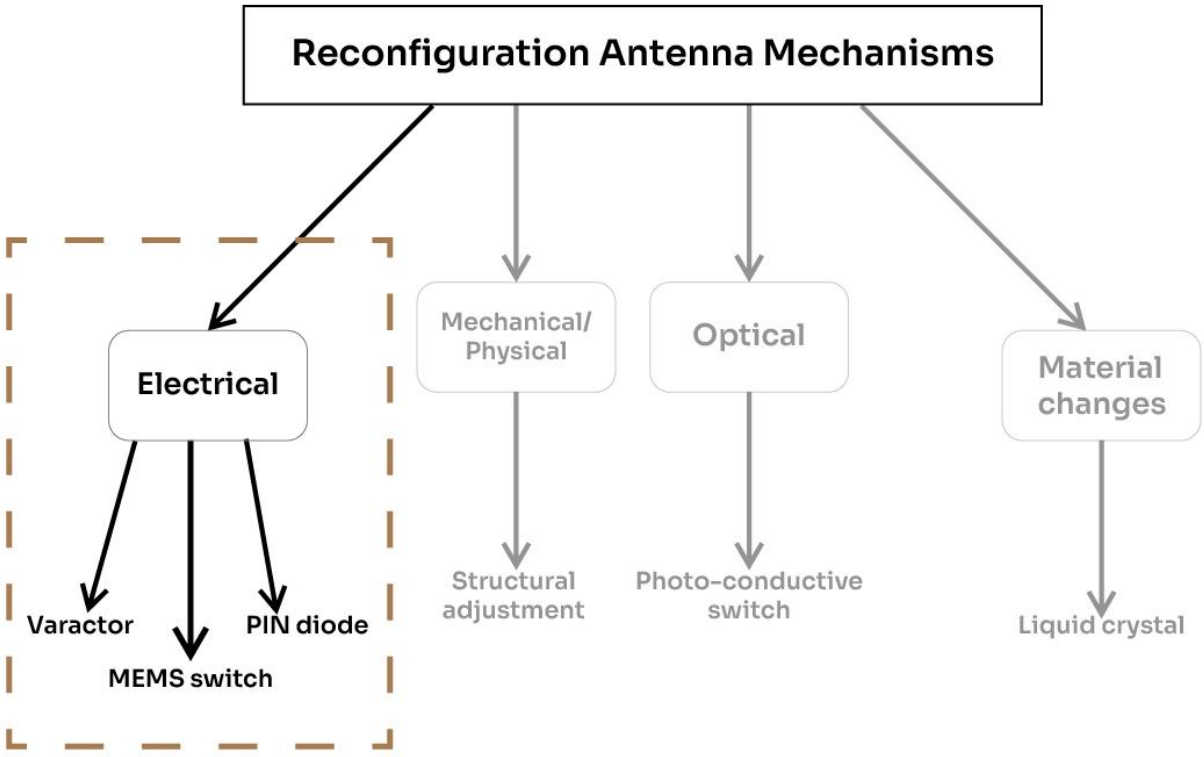

Figure 2.2: Reconfiguration antenna mechanisms.

2.3.1 Radio-Frequency MicroElectroMechanical System (RF MEMS) switch

A RF MEMS switch is a standard mechanical semiconductor-based switching system based on VLSI circuit fabrication technology. Basically, the switch involves a microelectromechanical movement controlled by electronic components to provide the switching functionality at radio frequencies. In an antenna design, the RF MEMS switch can be used to control the surface current flow either through short circuit or open circuit operation. In addition, a RF MEMS switch can be fabricated directly onto the antenna structure, i.e. printed on a glass or ceramic dielectric substrate. Figure 2.3 shows an equivalent circuit model and an example of RF MEMS switch. Since the device has low up state capacitance, this results in wideband performance in the antenna design. The typical advantages of RF MEMS switches are their low power consumption and high tuning speed (from 1 − 100 ns), low cost, high isolation and low insertion loss. However, the switch has limitation in poor quality factor, nonlinear behavior, non-continuous tunability and high DC bias current requirement in the “ON” state.

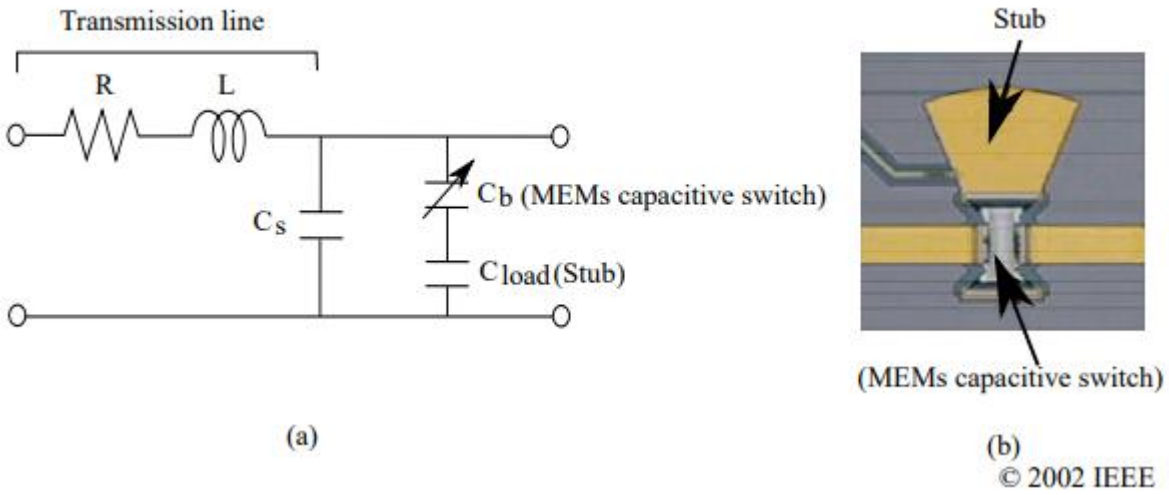

Figure 2.3: RF MEMS.

2.3.2 PIN Diode

A PIN diode is a semiconductor component including P-type and N-type regions, separated by an Intrinsic region. A PIN diode provides the ability to control low to high RF signals in different applications with a low level of DC biasing. The diode can be a good RF switching mechanism that can be integrated into the antenna design. It enables two modes of operation that will let RF signals pass or block them. The diode is in “ON” state when it is in forward bias DC current, and in “OFF” state when the diode is on reverse bias DC current. Figure 2.4 illustrates a PIN diode fundamental model and equivalent circuit in two mode of operations. The main advantages of the PIN diodes are their low DC actuation voltage combined with high tuning speed (1 − 100 ns), high-speed response, and a high reliability since they include no moving parts. Their simplicity and wide availability results in a low cost of production. The disadvantages of the PIN diode are non-continuous tunability and high reverse recovery time due to power loss.

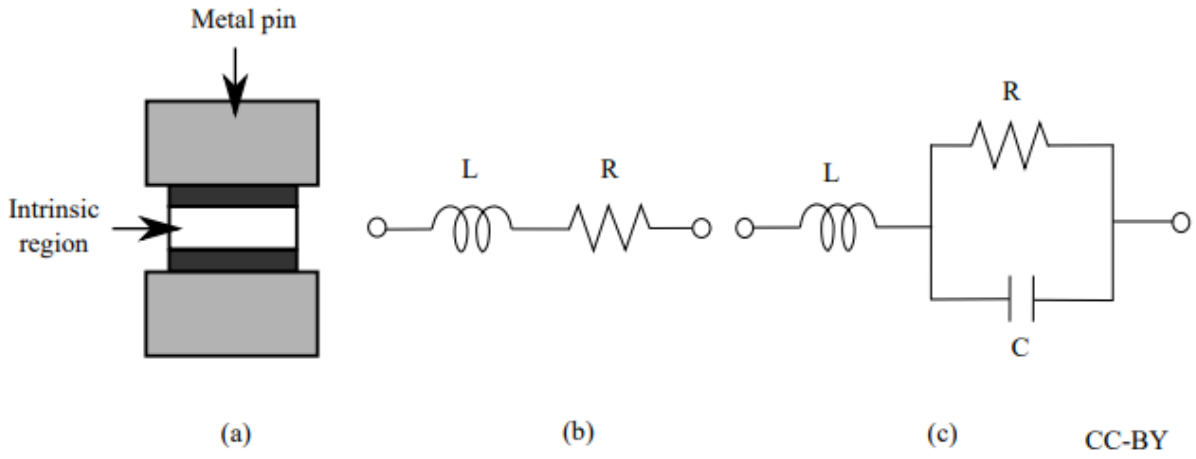

Figure 2.4: PIN Diode.

2.3.3 Varactors

A varactor diode (also sometimes referred to as varicap diode) is a semiconductor component that normally consists of a P-N junction. The varactor is considered as a special type of diode which provides a variable junction capacitance controlled by a bias voltage. Generally, the values of the variable capacitance can be up to tens or even hundreds of picofarads depending on the type and model of varactor [9]. The operation of the varactor is relying on the reverse biased state voltage and therefore nearly no DC current will flow through the component. Figure 2.5 shows an equivalent circuit of a varactor diode [10]. According to an example of a varactor datasheet [11], the variable junction capacitance C(V) can be calculated as:

$$C(V) = C_{JO}(1 + V/V_J)^M + C_{par} \quad (2.1)$$

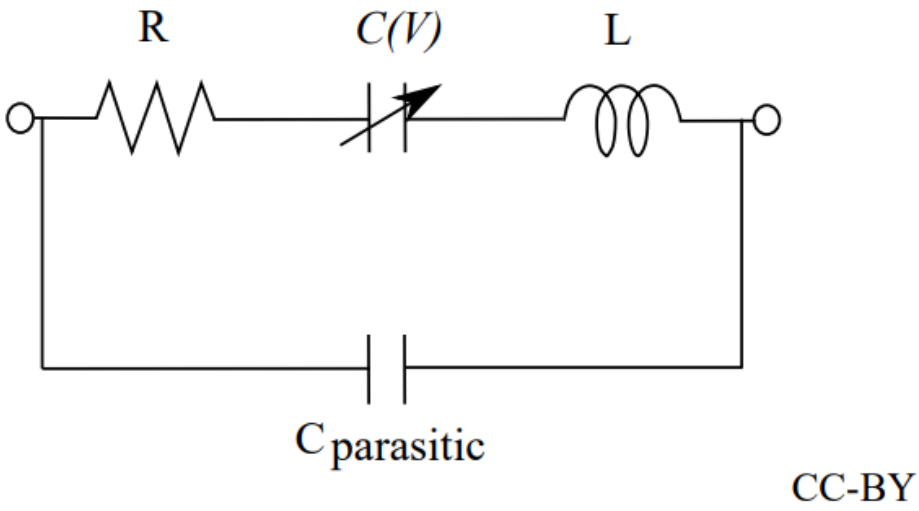

Figure 2.5: Varactor.

Where C_{JO} is the hyper abrupt junctions' capacitance, V_J is the built-in potential voltage, M is parameter of the abrupt junction and C_{par} is the parasitic capacitance of the varactor.

2.4 State of The Art of Reconfigurable Antennas

This section introduces the fundamental approaches to reconfigurable antenna technology, putting emphasis on electrically tunable implementations with diodes and switches as described in the previous section. It begins with a detailed explanation and summary of reconfigurable properties with some examples from the literature. For each modality of reconfiguration, the selected examples will sequentially cover actuation using RF MEMS, PIN diodes or varactors.

2.4.1 Frequency-reconfigurable Antennas

The frequency reconfigurability of the antennas can be implemented with the mentioned electrical tuning elements (RF MEMS switch, PIN diode and varactor) to attain a reliable system performance.

- **RF MEMS Frequency-reconfigurable Antenna**

An example in [12] proposed a reconfigurable RF MEMS integrated antenna with the ability to achieve two frequency modes of operation. A RF MEMS is embedded at a strategic location in the bottom layer of the antenna geometry, allowing to change the current path between a meander and a T-shaped structure. Figure 2.6 shows the photographs of the frequency-reconfigurable antenna operated by “ON” and “OFF” state of the RF MEMS switch. The antenna provides two modes with central frequencies of 0.718 GHz and 4.96 GHz. Another example was presented by [13] who proposed a reconfigurable patch antenna with RF MEMS switches directly integrated onto the patch antenna to provide three reconfiguration states of operation frequencies. The antenna supports frequency in low-band, mid-band and high-band at 1.16 GHz, 1.28 GHz and 1.6 GHz, respectively which are appealing to different applications.

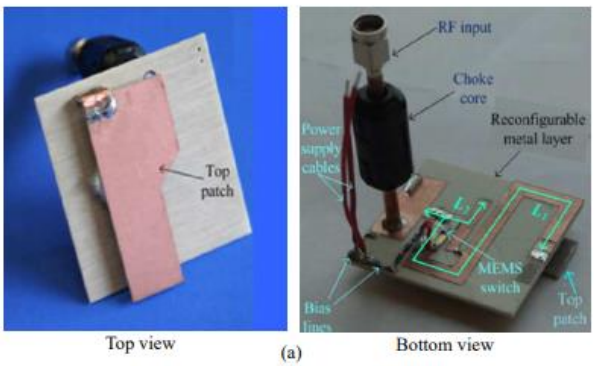

Figure 2.6: Example of RF MEMS frequency-reconfigurable antenna.

- **PIN diode Frequency-reconfigurable Antenna**

The use of PIN diodes as a switch for frequency reconfiguration has been extensively explored in the literature. For example, in [14] , a reconfigurable slotted rectangular compact patch antenna with a set of PIN diode working as switches is presented. The operation of the antenna is controlled based on the ON-OFF states of three switches that provide switchable sub bands between two single-band modes (2.3 and 5.8 GHz) and two dual-band modes (2.3/4.5 GHz and 4.5/5.8 GHz). With a similar operating principle, another example is found in [15], who also presented a wide range of frequencies that can be modified extensively, with three switchable multiband frequency response at 2.3 − 2.51 GHz, 3.35 − 3.75 GHz and 4.95 − 5.53 GHz for Bluetooth, WiMaX and WLAN applications, respectively. Another impressive design of frequency tuning reconfiguration is demonstrated in [16], where a rectangular microstrip patch antenna including a slot with optimized shape and switchable PIN diodes in the ground plane was proposed to increase reliability performance. There were two categories of antenna designs in this paper: Firstly, a design with a single diode mounted in the antenna structure had an “OFF” state corresponding to a frequency with higher priority. Secondly, with an increase to three diodes in the optimized structure, the reliability of the antenna was improved by adding four different switchable band of operations. The manufactured antenna and tunable frequencies of the antenna are shown in Figure 2.7, with a performance validating the concept.

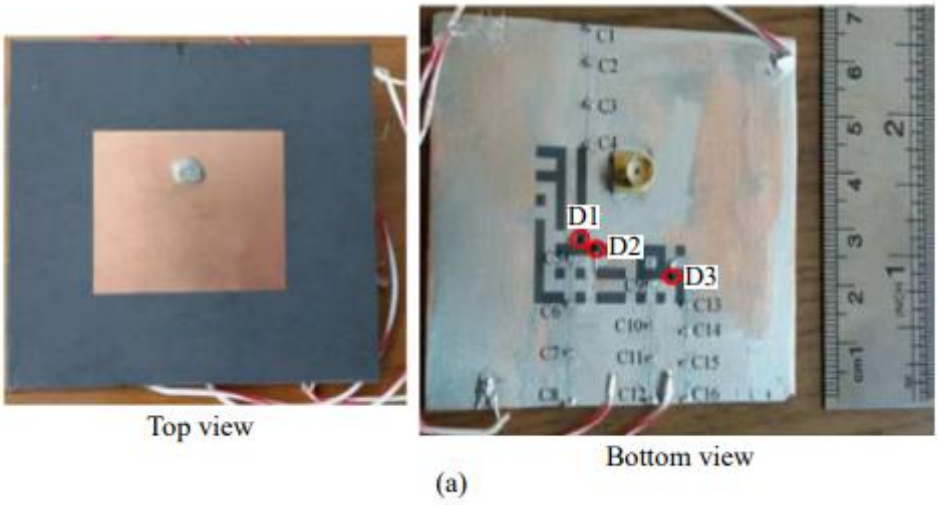

Figure 2.7: Example of PIN diode frequency-reconfigurable antenna.

- **Varactor-controlled Frequency-reconfigurable Antenna**

The integration of varactor diodes in frequency-reconfigurable antennas can be found in numerous publications. In [17], the variable capacitance from two sets of varactors was selected as tuning mechanism that independently controls the resonance frequencies in two distinct bands for a low-profile monopolar antenna. In this case, the antenna provided continuously tunable dual-frequency bands. The lower band was achieved by an equivalent magnetic-current loop through a center-fed patch with shorting rods. Then, four symmetrical slots on the patch created another magnetic-current loop that define the radiation in the upper band. Figure 2.8 shows the examples of the reconfigurable antenna, together with the frequency reconfigurable reflection coefficient.

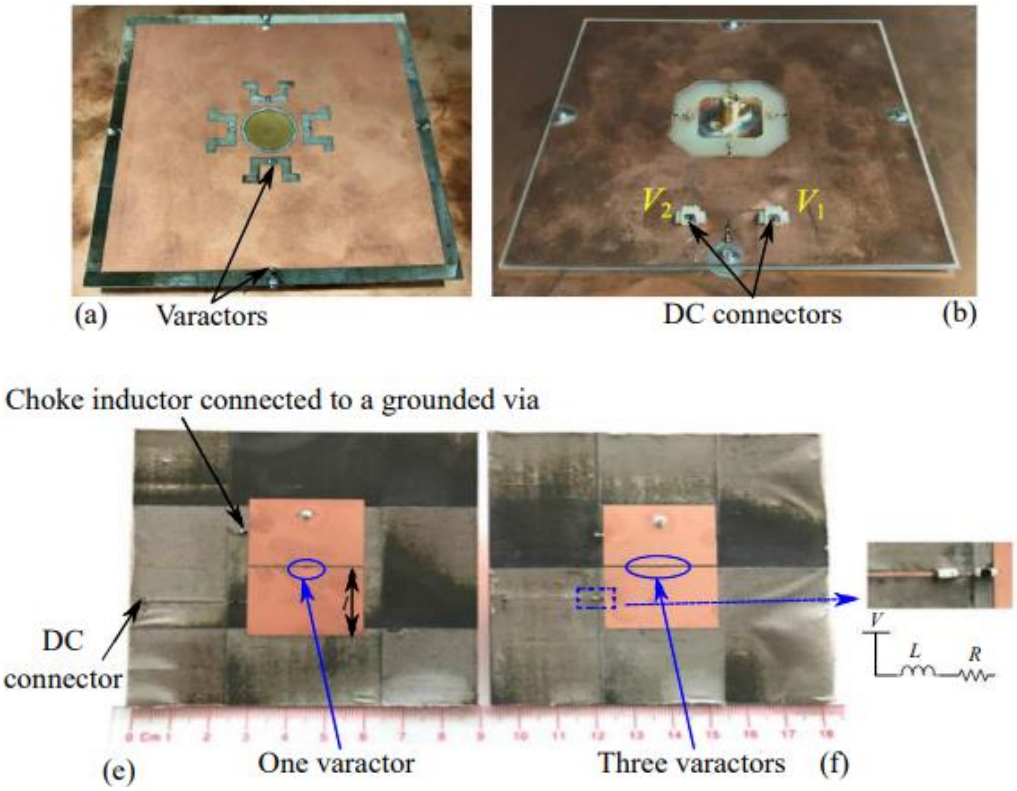

Figure 2.8: Examples of varactor-controlled frequency-reconfigurable antenna.

2.4.2 Radiation Pattern-reconfigurable Antennas

In general, electrical changes to a radiating structure usually result in changes in radiation characteristics. Knowledge of the fundamental operation of the antenna in question can help to make the appropriate changes to arrive at a useful design. For example, reconfigurable radiation patterns can be achieved with slot-based radiators. As in the examples above, an annular slot antenna is used as both a frequency- and pattern-reconfigurable device. Frequency reconfigurability for this antenna is supported through, a PIN diode for example, which switches that control input matching circuitry, whereas the pattern reconfigurability is enabled with diode switches placed at locations around the slot to control the direction of a pattern null that is inherent to basic antenna operation. And there are so many other ways to perform the pattern-reconfigurability, like:

2.4.2.1 Parasitic Tuning

Microstrip-based reconfigurable antennas can also use switched or tuned parasitic elements, one example is that developed by [18] Shown in Figure 2. (a), the antenna is composed of a single linear element with two spaced parasitic elements positioned parallel to the driven element. Parasitic element lengths are changed with electronic switches or varactors, which, in turn, alter the magnitudes and phases of the currents on the parasitic elements relative to the driven element. Tilts in the main beam in one plane can then be switched or swept as the lengths of the parasitic elements are changed. A photograph of the antenna is shown in Figure 2.9 (b) equipped with PIN diode switches. Note the careful design of the switch control circuitry shown in Figure 2.9 (b) that minimizes the effects of radiation from DC bias lines. With the driven element relatively isolated from the reconfigured sections of the structure, the operating frequency and impedance bandwidth are preserved. This antenna, in a similar manner to most parasitically tuned antennas, can be analyzed theoretically using a combination of coupling and array theory to explain pattern tilts. For tuned parasitic systems such as these, search and optimization algorithms can be used to determine the tuning reactance necessary on each parasitic element to produce a beam or null at a prescribed angle [19].

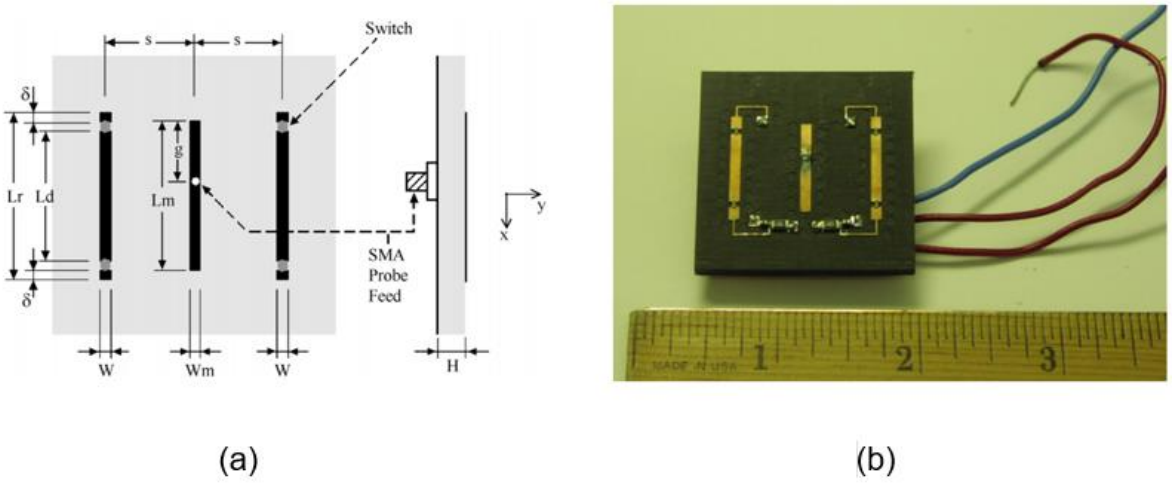

Figure 2.9: (a) Physical structure and parameters of the reconfigurable microstrip parasitic array, (b) Photograph of the reconfigurable microstrip parasitic array.

2.4.2.2 Array Tuning

Integrating phase shifts into array element reconfigurability can result in beam steering similar to that achieved with traditional phased arrays but without the inherent costs of phase shifters. Several reconfigurable apertures and surfaces based on this principle are discussed here. One approach to achieve radiation pattern reconfiguration uses phased-tuned reflect array elements. In this work, an electronically scanned reflect array uses reconfigurable microstrip patch antenna elements to vary the reflection phase across the array. The reconfigurable element, shown in Figure 2.10, is a simple microstrip patch element with aperture coupling to a transmission line loaded with two varactor diodes. By varying the bias across the two varactors, each element reflection phase can be varied over 360°, which supports array beam steering to up to 40° from broadside with a 30-element array [19].

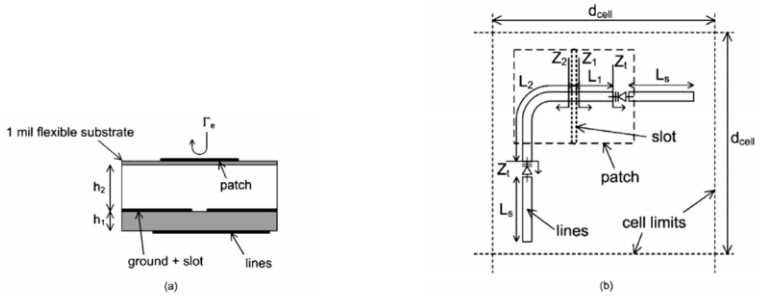

Figure 2.10: Reconfigurable reflect array element (a) side view and (b) bottom view.

2.5 Stat of the art of reconfigurable Antennas in Ku band

The Ku Band has been used for many years in different companies and its usage was generalized with the appearance of the VSATs (Very Small Aperture Terminal) thanks to two great benefits, on the one hand, its frequency range allows to achieve high and on the other hand, for its performance a small equipment is used, which reduces its complexity and logistic cost as well as the installation of the services. Some uses and applications of this frequency band are:

The Ku band is mainly used for satellite communications, especially downlink, used by direct-transmission satellites for satellite television and specific applications such as the NASA's Tracking Data Relay Satellite used for both the space shuttle and for communications from the International Space Station (ISS).

While the Ku frequency band is recommended for any sector that requires high bandwidth, it is suggested to apply it to the oil, financial, mining and energy sectors. For that, satellite antenna manufacturers work to renew the power with which the signal is received on the ground, to cover the needs and conditions of each of these economic sectors.

A major attraction of the band over lower frequency microwave bands is that the shorter wavelengths allow sufficient angular resolution to separate the signals of different communication satellites to be achieved with smaller terrestrial parabolic antennas.

The Ku band also offers a user more flexibility. A smaller dish size and a Ku band system's freedom from terrestrial operations simplifies finding a suitable dish site. For the end users Ku band is generally cheaper and enables smaller antennas (both because of the higher frequency and a more focused beam). Ku band is also less vulnerable to rain fade than the Ka band frequency spectrum.

Some of the many applications used within the Ku band are presented down below.

The following designed antenna is suitable for the 12 GHz Broadcasting Satellite Service (BSS) frequency bands [20]. It is working in the frequency band 12.43–12.53 GHz. A single-feed planar antenna can be easily integrated. The antenna consists of 32-elements with corporate feeding network. This feeding was designed to give equal amplitude and phase to each element.

The fabricated patch is shown in Figure 2.11. The array was fabricated on a dielectric substrate called Teflon with h = 0.7874 mm, ε_r = 2.2, area of 91.5 × 53 mm. The dimension of the patch and the spacing between the elements in x and y directions are 9.5 × 7.6, 12.0482, and 12.0482 mm respectively. The feeding system includes three different microstrip transmission lines of different impedances and different widths. The impedances are 50 Ω, 71.7 Ω, and 100 Ω and the corresponding widths are 2.377 mm, 1.339 mm, and 0.655 mm respectively.

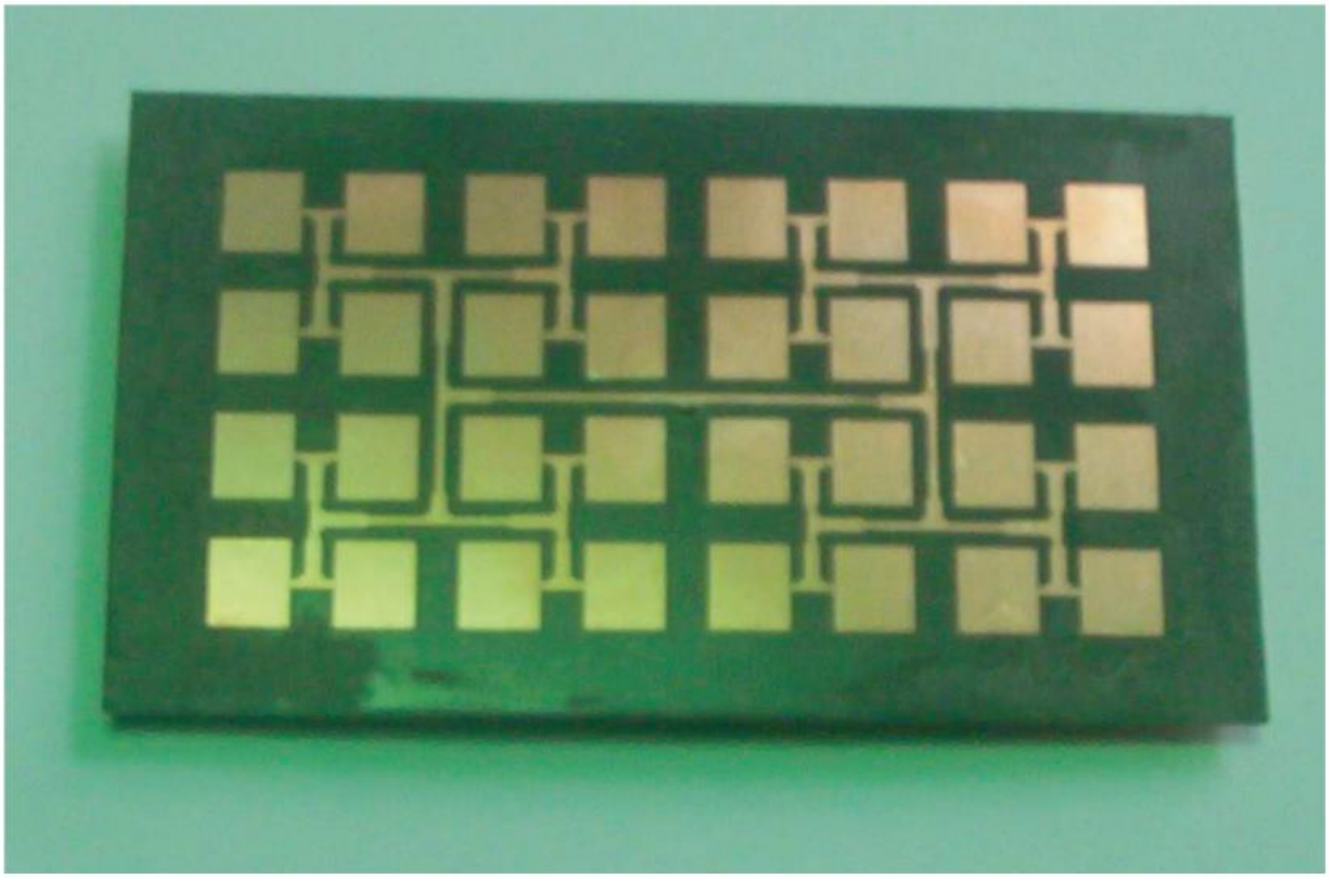

Figure 2.11: *The fabricated array antenna [20].*

In [21], a simple and low-cost approach to implement dual-band dual-CP array is proposed. The RHCP/LHCP (Right Hand Circular Polarized/ Left Hand Circular Polarized) is achieved by connecting two patches working at two different frequencies and different polarizations directly. The design freedom is enhanced by this method. The CP sense and the frequency ratio can be adjusted easily. Since the element is fed by microstrip line, it can be extended to a larger array easily. Dependent on the feed network used, the dual-band dual-CP element can be extended to different kinds of arrays. To show the benefits, two kinds of feed networks are present in this paper. One is using the conventional feed network, and the other is using the sequential rotation technique to enlarge the 3-dB axial ratio (AR) bandwidth.

The element structure is shown in Figure 2.12. Two single-feed CP patches are connected at point O. The patches are designed to realize RHCP and LHCP at frequencies $f_1 = 12.17\ Ghz$ and $f_2 = 17.5\ Ghz$ $(f_1 < f_2)$, respectively. CP is achieved by cutting thin slots at the center of square patches. The width of the total element w is 13.4 mm and the distance between these two patches d_3 is 1.3 mm.

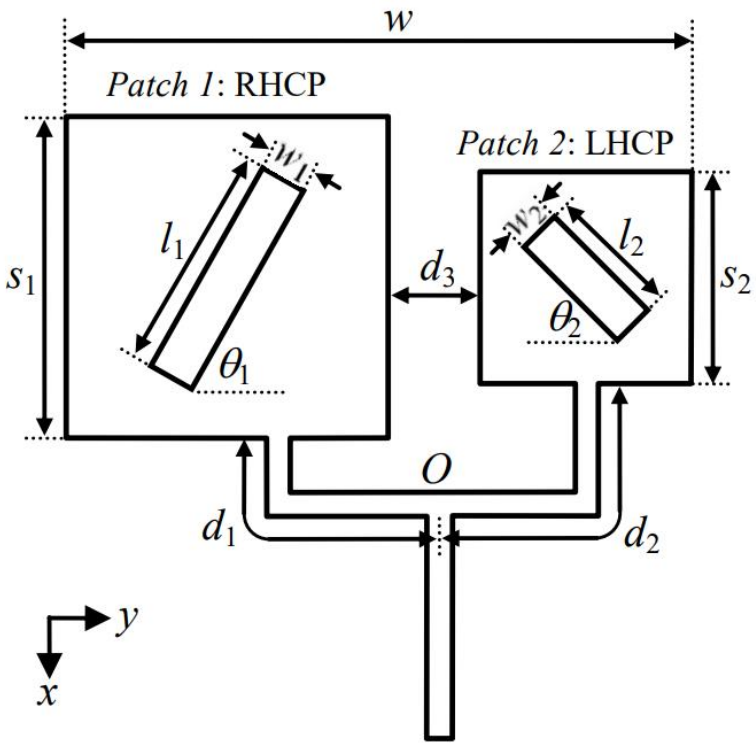

Figure 2.12: *Structure of the dual-band dual-CP element [21].*

A simple way to compose a large array is by using the conventional feed network. Take a 4×4-element array as an example, the structure is shown in Figure 2.13 (b). This array is composed of four 2×2-element subarrays as shown in Figure 2.13 (a). All the elements of each subarray are fed by a wide-band feed network, which is composed of three two-section T-junction power combiners and microstrip lines.

An effective method to enlarge the AR bandwidth is by using sequential rotation technique. Four same patches are rotated around a center point. The phases of these patches are set to be 0°, 90°, 180°, and 270°, respectively. The RHCP (LHCP) can be achieved when the phases increase gradually along the anti-clockwise (clockwise) direction. Through this method, the AR bandwidth can be much enlarged.

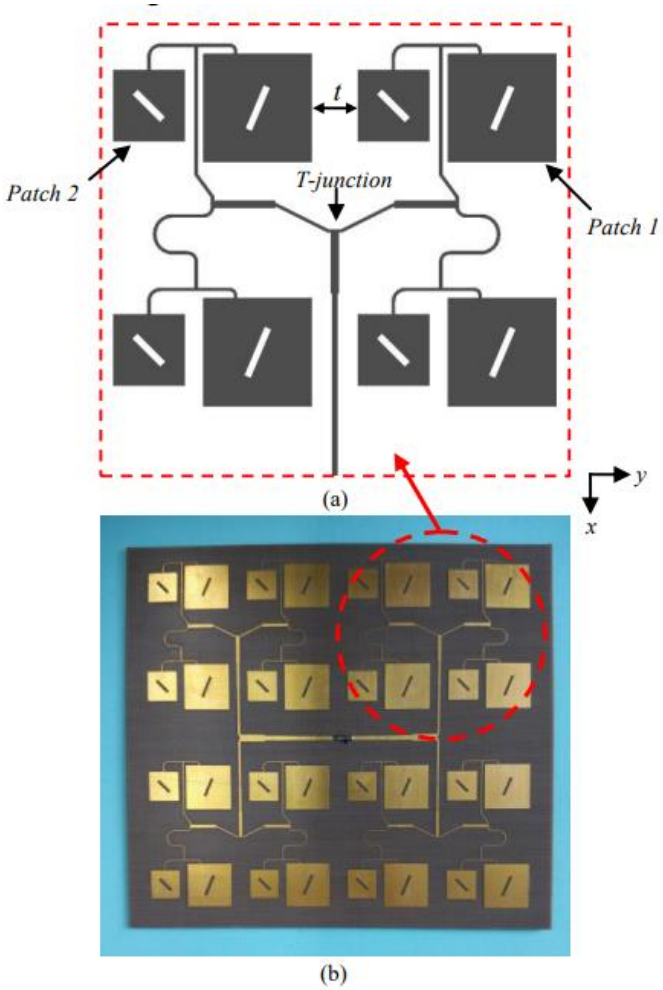

Figure 2.13: Structure of the dual-band dual-CP array with conventional feed [21].

In [22], the aim of this paper is to present a particular antenna structure, working as a transmit-array structure (reception/ transmission lens). Because of its working function, the structure consists of a patch array in the reception part, a phase delay for each patch and another patch array in the transmission part. The idea in using this lens is to place it in front of a particular antenna to modify the radiation pattern of the feeding antenna. The architecture which is being applied implies the use of patches with probe feeding.

The working frequency would be 12 GHz. The phase delay is obtained by adding pieces of 50Ω Strip line in the center of the structure as shown in Figure 2.14.

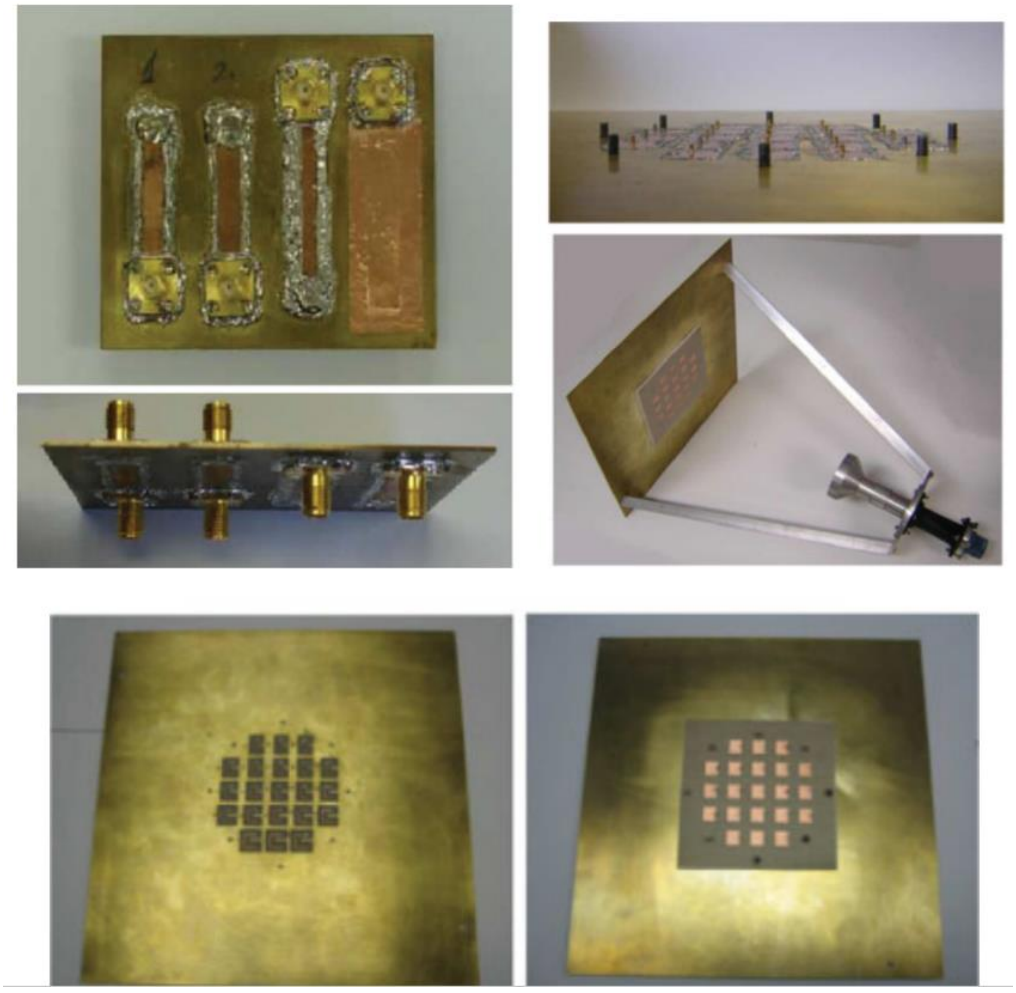

Figure 2.14: *Some photographs and details of the prototype [22].*

In [23], this paper presents a study, analysis of microstrip patch arrays for the 5G application. It is the analysis of two elements of microstrip patch designed at 12 GHz as shown in Figure 2.15. For better impedance matching, corporate feeding network is used in three configurations of an array. Microstrip line and patch are etched on RT Duroid 5880 (dielectric constant of 2.2 and a height of 1.56 mm) substrate material. Corporate feeding is modified and various performance parameters, namely, frequency and radiation pattern, were compared with conventional corporate feeding.

The geometry of two elements and its modified version and their radiation patterns are shown in Figure 2.15 (a), (b) and Figure 2.16 respectively.

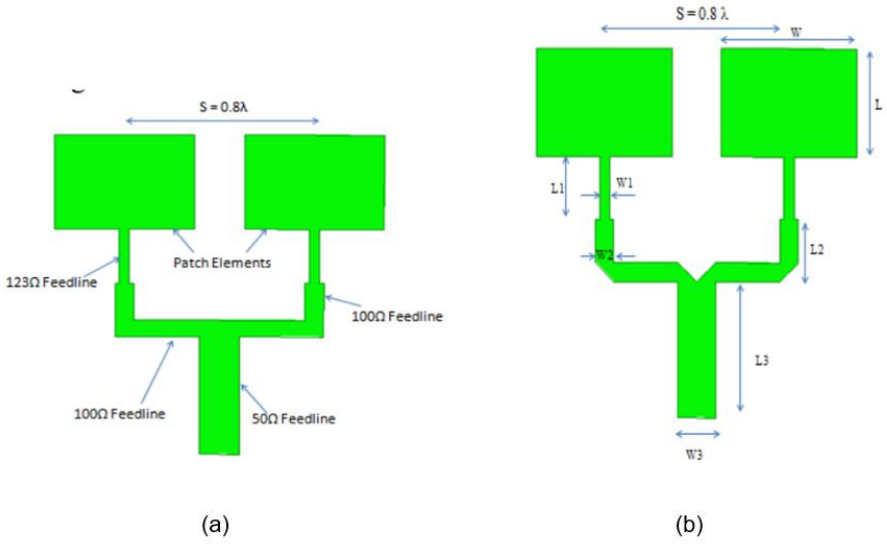

Figure 2.15: *(a) Geometry of conventional of two elements array with corporate feeding at 12 GHz, (b) Geometry of modified two elements array with corporate feeding at 12 GHz [23].*

Conventional configured antenna resonates at 12 GHz but at return loss of - 20 dB whereas the Modified array configured antenna resonates at 12 GHz at return loss of -38 dB. According to this analyzed result we can concluded that the modified configured array is better to use than conventional array.

Radiation pattern of the far-field at 12 GHz are shown in Figure 2.16. It has broad band and linear radiation pattern. Two element array antenna has 5.16 dB & 5.29 dB gain and directivity respectively.

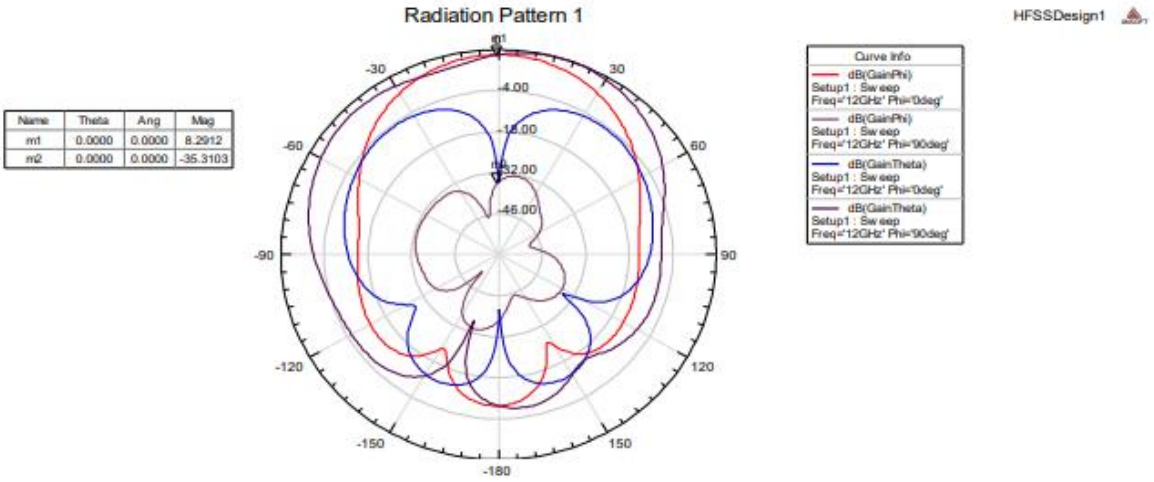

Figure 2.16: Radiation Pattern of Two elements array with modified corporate feeding at 12 GHz [23].

2.6 Conclusion

This chapter has presented reconfigurable antennas in the Ku band and their mechanisms to be reconfigured within that band, and also, it has had some works about their uses and applications in the telecommunication field.

Chapter 3

Design and Simulation of Two Elements Array Antenna for Ku Band

3.1 Introduction

This chapter starts by designing a single and two elements array antenna within the frequency of 2.4 GHz. Then, it presents the design of a single and two elements array antenna within the Ku band. The proposed designs can provide reconfigurability in their radiation characteristics by tuning capacitors values. The parametric studies on its structure geometry are done with CST Microwave Studio.

3.2 CST Microwave Studio

CST Studio Suite® is a high-performance 3D EM analysis software package for designing, analyzing and optimizing electromagnetic (EM) components and systems.

Electromagnetic field solvers for applications across the EM spectrum are contained within a single user interface in CST Studio Suite. The solvers can be coupled to perform hybrid simulations, giving engineers the flexibility to analyze whole systems made up of multiple components in an efficient and straightforward way. Co-design with other SIMULIA products allows EM simulation to be integrated into the design flow and drives the development process from the earliest stages [24].

3.3 Reconfigurable Two-Elements Array Antenna for 2.27 GHz

3.3.1 The Design Procedure for a Single Element Antenna for 2.27 GHz

Given that the main design is based on a resonant patch, the first step requires defining the patch dimensions, selecting the appropriate material and substrate thickness. Figure 27 shows the single-element antenna geometry. For this design, Rogers Duroid 5880 is selected as dielectric substrate with a relative permittivity of 2.2, loss tangent of 0.0009 and thickness of $1.578\ mm$.

For the designing of Microstrip patch antenna, a Dielectric substrate and Resonate frequency have to be chosen by using the parameters which can be found out by the equations below [5]:

$$W = \frac{c}{2f_r}\sqrt{\frac{2}{\varepsilon_r+1}} \qquad (3.1)$$

Where W is the width of the patch.

f_r is the resonate frequency.

c is free space velocity.

ε_r is the Dielectric constant of substrate.

$$\varepsilon_{reff} = \frac{\varepsilon_r+1}{2} + \frac{\varepsilon_r-1}{\sqrt{1+12\frac{h}{W}}} \tag{3.2}$$

With $\frac{h}{W} > 1$, and

h is the height of the Dielectric substrate.

ε_{reff} is the effective Dielectric constant of substrate.

$$\frac{\Delta L}{h} = 0.412\frac{(\varepsilon_{reff}+0.3)(\frac{W}{h}+0.264)}{(\varepsilon_{reff}-0.258)(\frac{W}{h}+0.8)} \tag{3.3}$$

Where ΔL is the length extension.

$$L = \frac{c}{2f_r\sqrt{\varepsilon_r}} - 2\Delta L \tag{3.4}$$

Where L is the actual length of the antenna.

$$W_g = 6h + W \tag{3.5}$$

$$L_g = 6h + L \tag{3.6}$$

Where W_g is the width of the ground plane, and L_g is its length.

Using the former mentioned equations, we find the dimensions as; $L_p = 41.1\,mm$ and $W_p = 49.5\,mm$, yielding a resonance frequency of 2.27 GHz. The figure 3.1 shows the design of this single element.

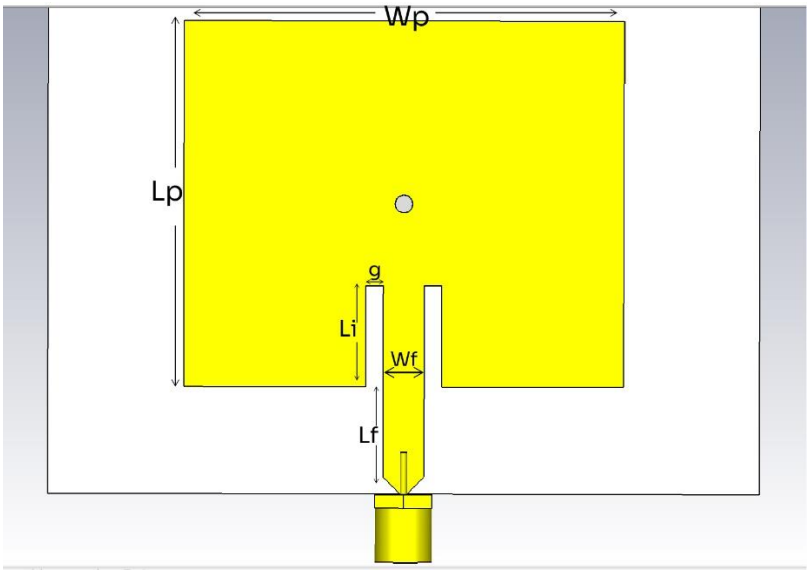

Figure 3.1: Single-element of 2.27 GHz.

The inset feed arrangement with line width $W_f = 4.6\,mm$, $L_f = 12\,mm$, gap $g = 2\,mm$ and position $L_i = 11.4\,mm$ is optimized to provide impedance matching between the antenna and a 50Ω feed network, with a short trimming from both sides of the feedline to prevent the contact of its metallic side with the one of the connector. (Figure 3.2)

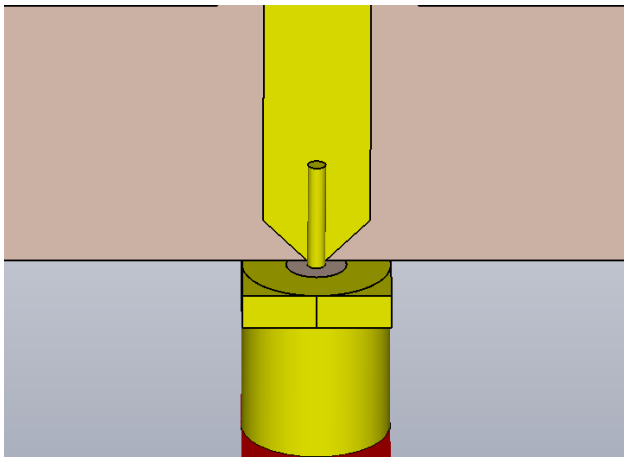

Figure 3.2: Trimmed feedline.

A shorting-via is added to the antenna afterwards, its main objective is to make a contact point of the patch itself with the ground plane. The positioning of the shorting via was chosen by picking the middle point and changing it accordingly, the results of the reflection coefficient of each side can be found in the Figure 3.3. Where Y is the actual center point of the pitch. That exact same point of the patch was picked for being the closest result to the resonance frequency. The variation of via's position leads to a frequency shift.

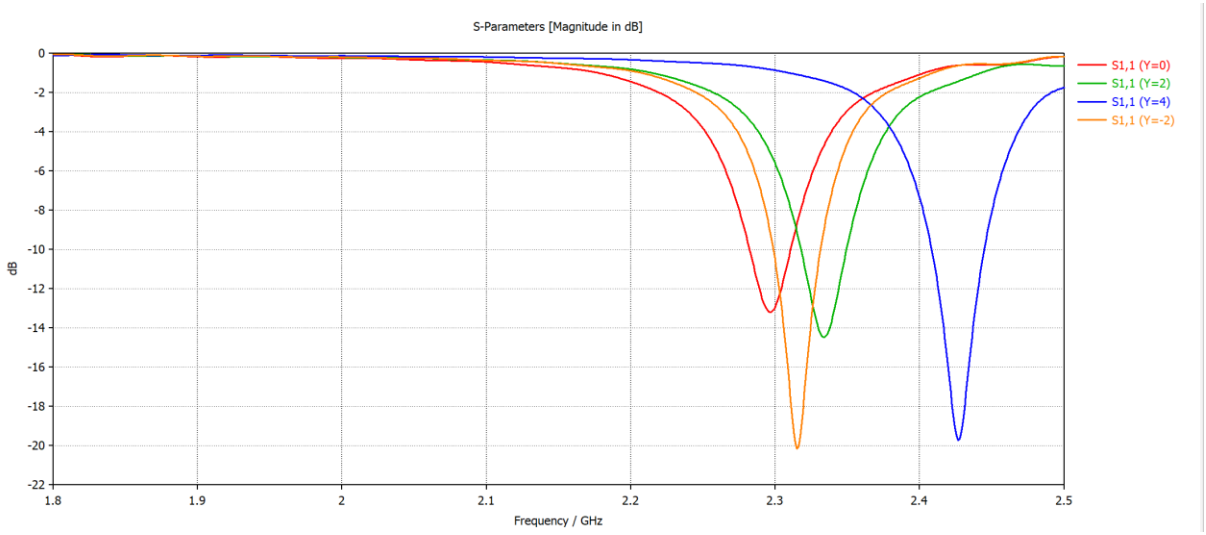

Figure 3.3: Reflection coefficients for different values of Y.

Figure 3.4 presents the reflection coefficient of the single element without any configuration applied to it at the resonance frequency.

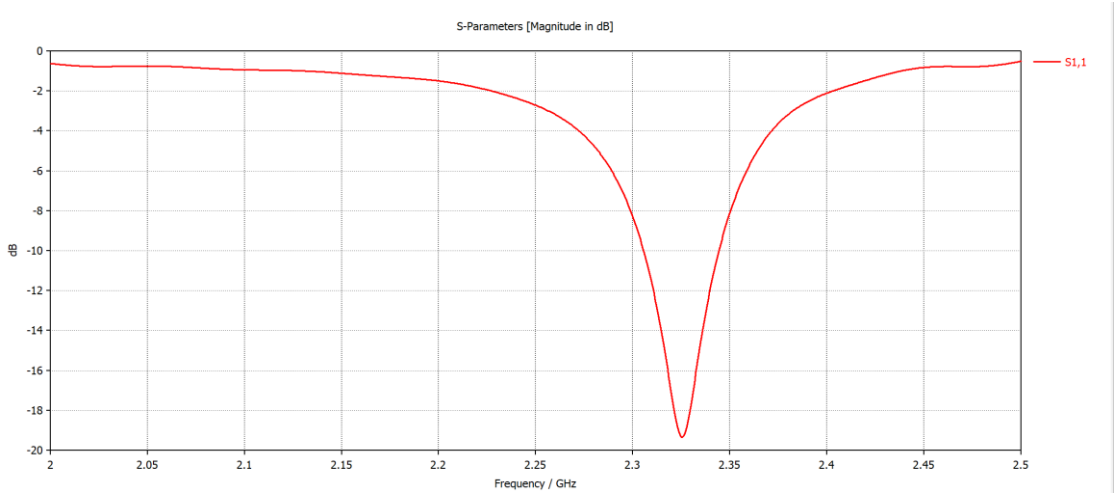

Figure 3.4: The reflection coefficient for a single element.

To introduce reconfigurability, firstly, a stub has to be added, as shown in Figure 3.5, to maintain the resonance after adding a capacitor to this patch. The stub's dimensions were picked according to its best reflection coefficient result. Some samples of the results of it while its reconfiguration are shown in the Figure 3.6.

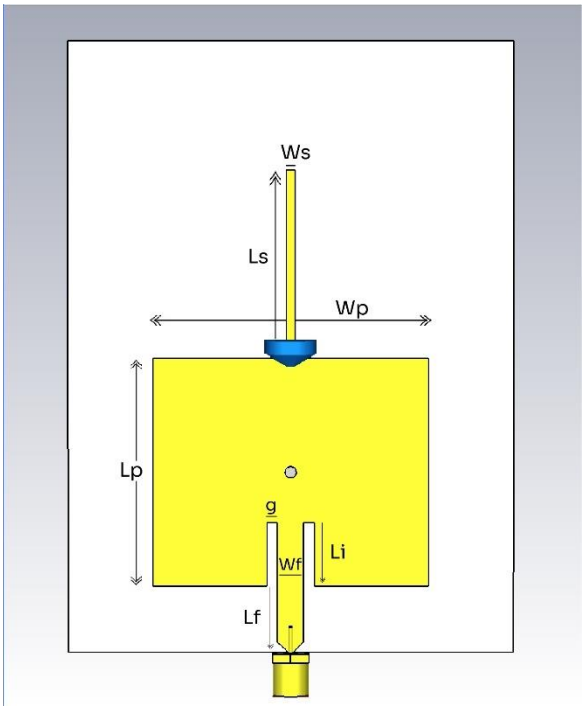

Figure 3.5: Single-element configuration.

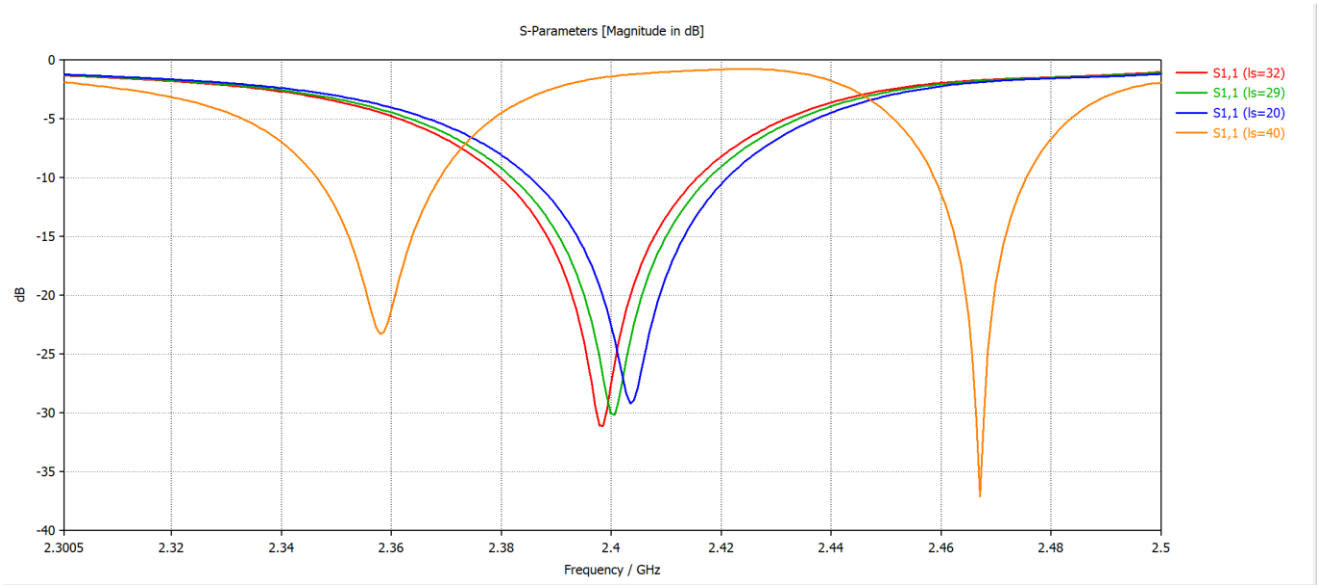

Figure 3.6: Reflection coefficients for different values of L_s.

The final dimensions of the stub are $W_s = 1.5\,mm$ and $L_s = 32\,mm$. Now, the varactor is added to the patch to enable reconfigurability,

Figure 3.7 shows the tuning range of the single element's resonance frequency at different varactor capacitance values ranging from 0.149 pF to 1.304 pF.

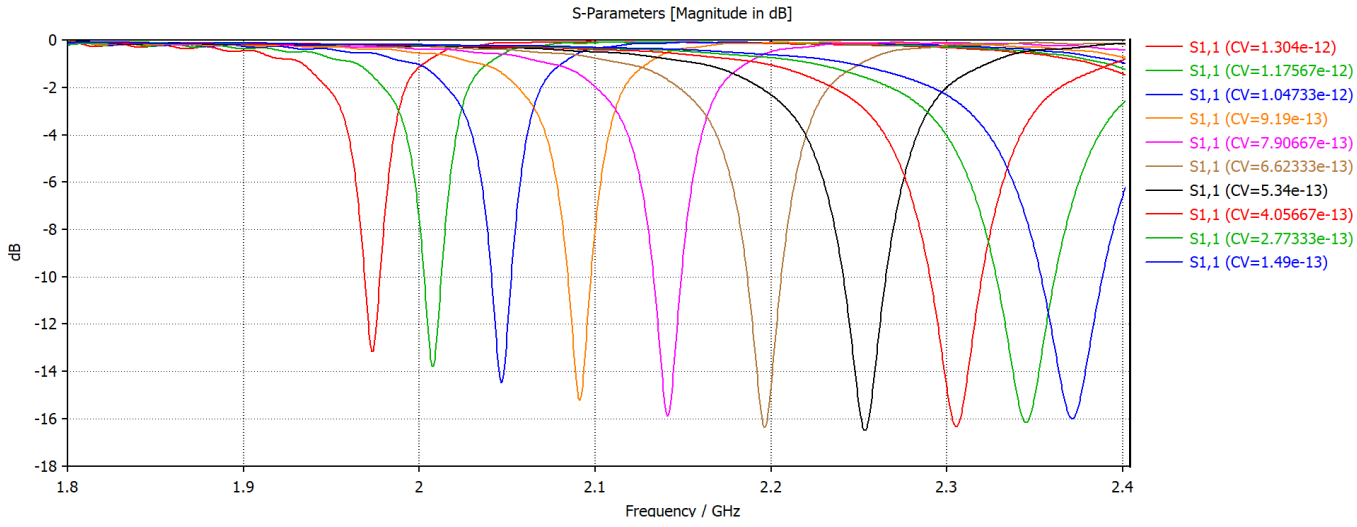

Figure 3.7: The tuning range of the resonance frequency.

After finally picking the right capacitance value of $C = 0.149\ pF$, and the dimensions of the patch which are $L_p = 41.1\ mm$, $W_p = 49.5\ mm$, $W_f = 4.6\ mm$, $L_f = 12\ mm$, gap $g = 2\ mm$, $L_i = 11.4\ mm$, and for the stub $W_s = 1.5\ mm$ and $L_s = 32\ mm$, the reflection coefficient is show in Figure 3.8.

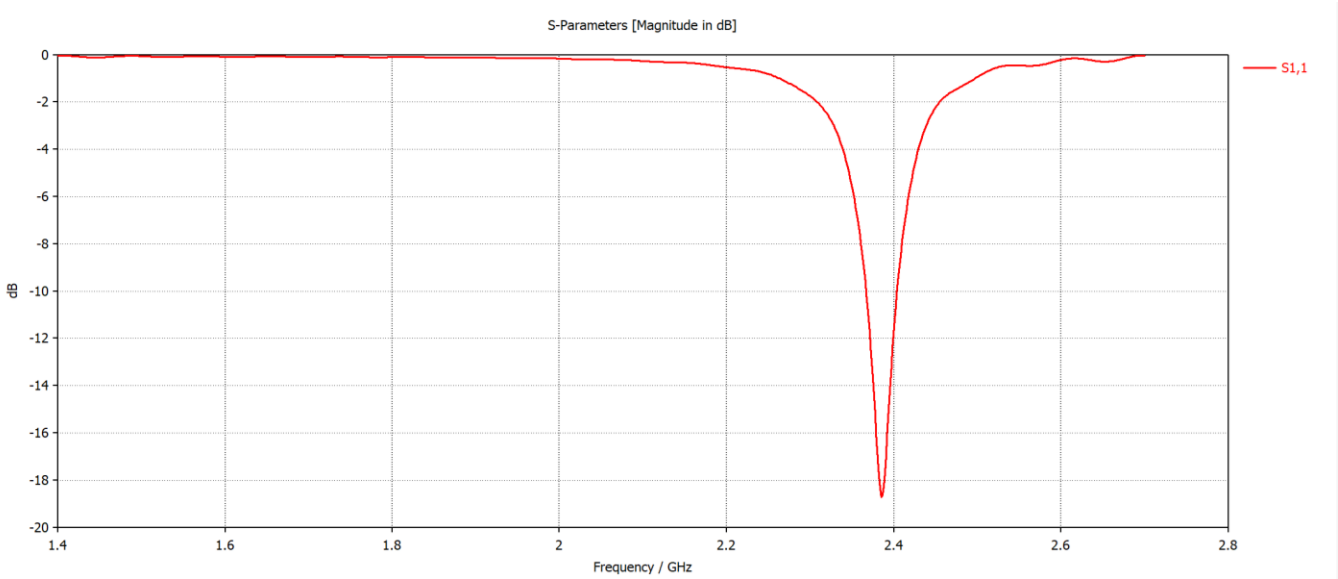

Figure 3.8: *Reflection coefficients for antenna with* $C = 0.149\ pF$.

3.3.2 The Dephasing Principal

In the proposed geometry, the phase difference between the two elements is obtained by adjusting the effective electrical length of the individual patches through variation of the varactor capacitance. As a starting point, a particular resonance frequency $f_0 = 2.27\ GHz$ can be tuned by adjusting the varactor capacitance $C_0 = 0.49\ pF$. Then, if a slight capacitance variation $\pm\Delta C_0 = 0.033\ pF$. is introduced for the two elements (one positive, one negative), selected by the actual bandwidth of the accepted $f_0 = 2.27\ GHz$ values, (starting from -10 dB), the patches become slightly detuned from their resonance. As the result, the introduced non-zero reactance at $f_0$cause a relative phase shift between the two elements, while their magnitude remains nearly the same. In this scenario, a continuously steerable beam around broadside can be achieved, with this pattern reconfigurability covering the frequency tuning range. Figure 3.9 shows this actual example graphically. In fact, for $f_1 = 2.285\ GHz$, the value is $C_0 - \Delta C_0 = 0.457\ pF$ and for the frequency $f_2 = 2.255\ GHz$, the value is $C_0 + \Delta C_0 = 0.523\ pF$.

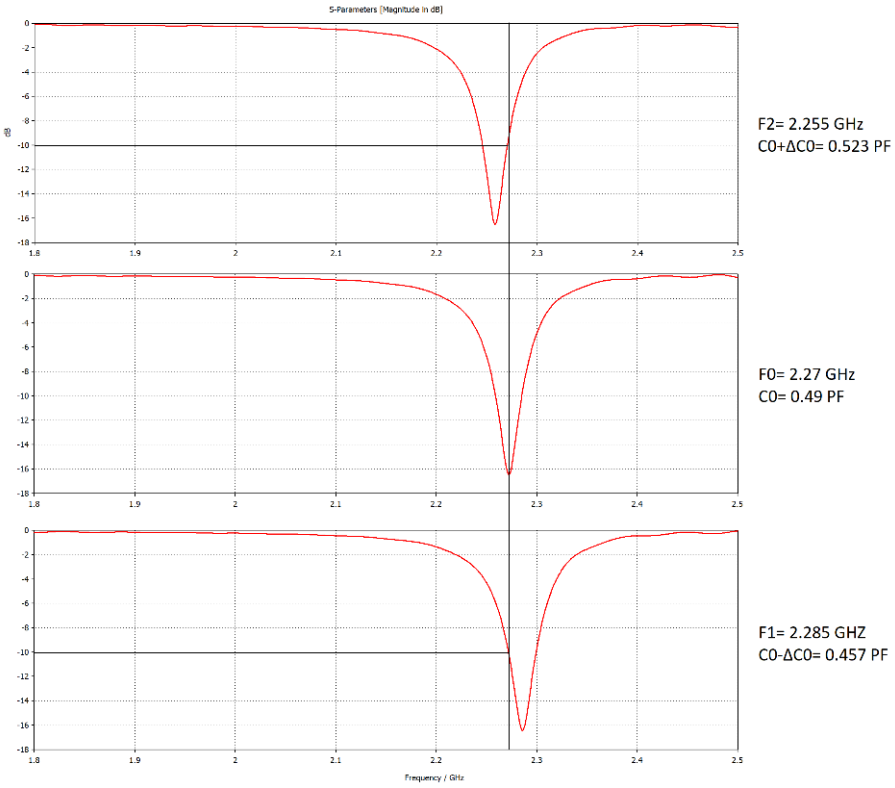

Figure 3.9: Reflection coefficients for different values of C; (a): $C = 0.523\ pF$, (b) $C = 0.49\ pF$, (c): $C = 0.457\ pF$

Figure 3.10 shows the current distribution on the patch for the 3 cases. We observe that, for the 3 frequencies: $f_0 = 2.27\ GHz$, $f_1 = 2.285\ GHz$ and $f_2 = 2.255\ GHz$, currents are spread out over the patch which prove operation at these 3 frequencies.

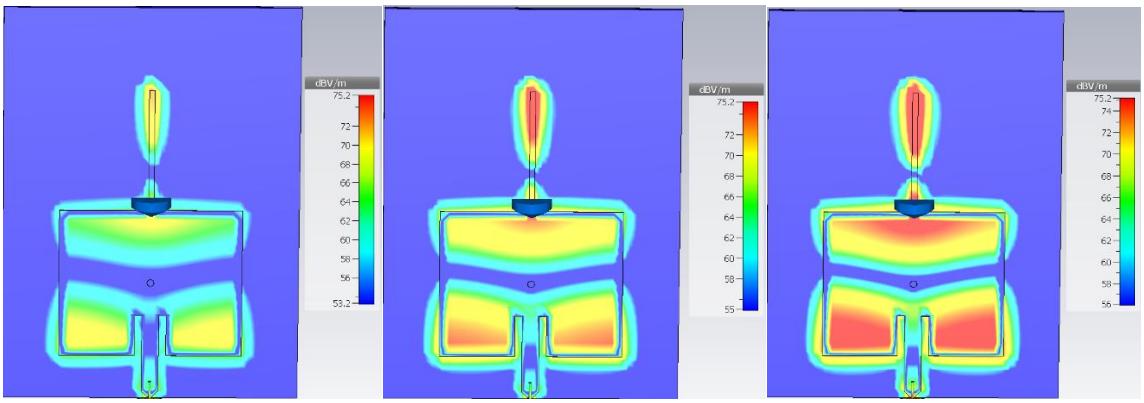

(a) (b) (c)

Figure 3.10: The current distribution on the patch for the 3 cases; (a): $f_2 = 2.255\ GHz$, (b): $f_0 = 2.27\ GHz$, (c): $f_1 = 2.285\ GHz$.

3.3.3 The Design Procedure for Two-Elements Array Antenna for 2.27 GHz

As shown in Figure 3.11, two reconfigurable patch elements with inter-element distance d_p are fed by a T-junction power divider by the dimensions of $L_f = 12\ mm$, $L_b = 14\ mm$ and $L_a = 33\ mm$, and a slightly different gap with $g = 3\ mm$ and $L_i = 13\ mm$. The feed network is designed with 50-Ω microstrip line, then divided up into two 100-Ω splitting in-phase feed lines. The size of the substrate is selected to $L_{sub} \times W_{sub} = 151.5\ mm \times 160.9mm$.

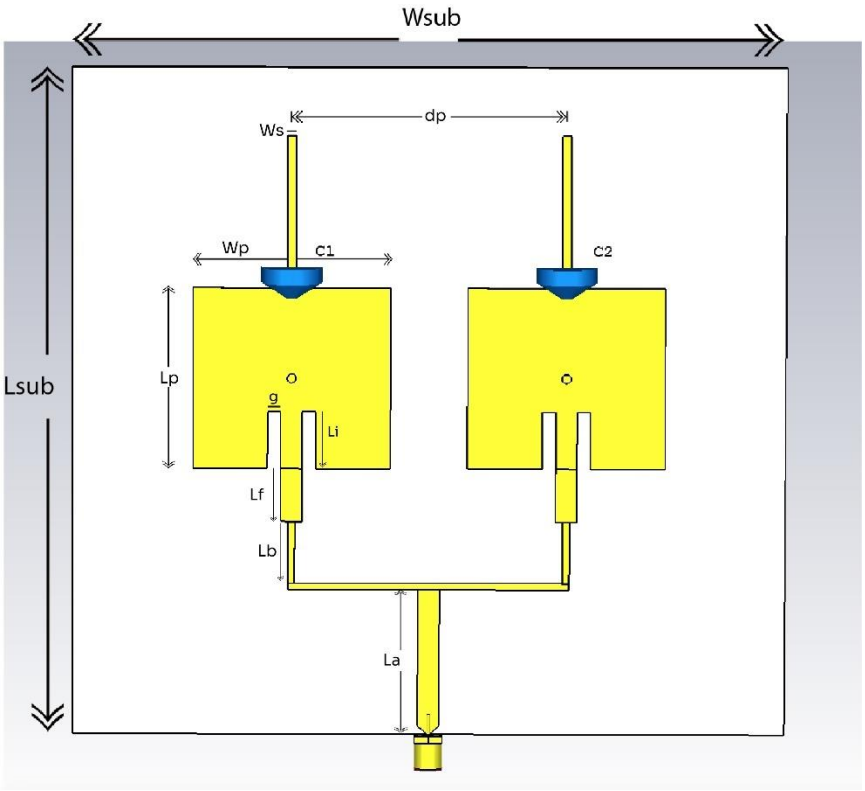

Figure 3.11: The reconfigurable two-element antenna configuration.

The distance between the 2 antennas d_p, the width L_b and the T-junction width W_s have been studied. Figures 3.12, 3.13 and 3.14 show the variation of S11 for the different values of d_p, L_b and W_s, respectively.

We observe a better impedance matching when d_p value decrease. On the other hand, the variation of either L_b or W_s has a little influence on the matching impedance.

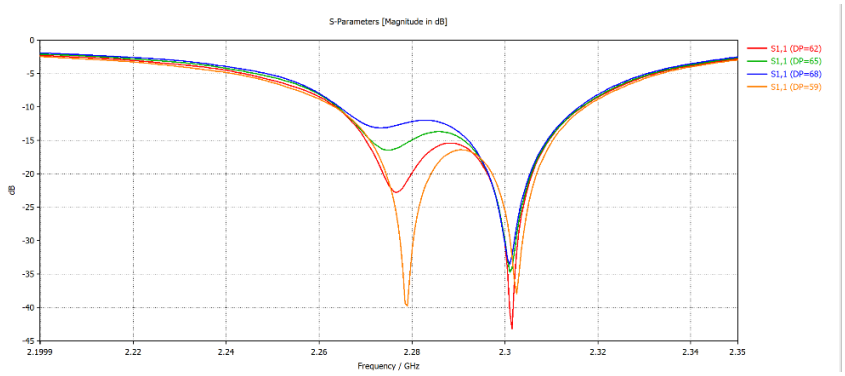

Figure 3.12: Reflection coefficients for different values of d_p.

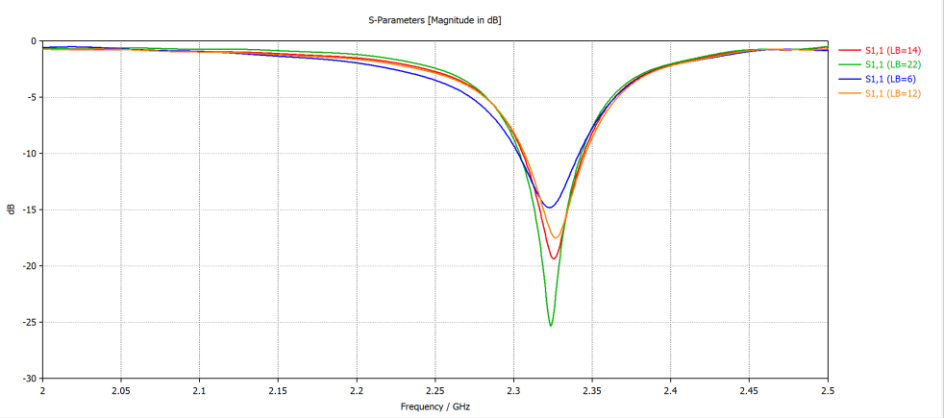

Figure 3.13: Reflection coefficients for different values of L_b.

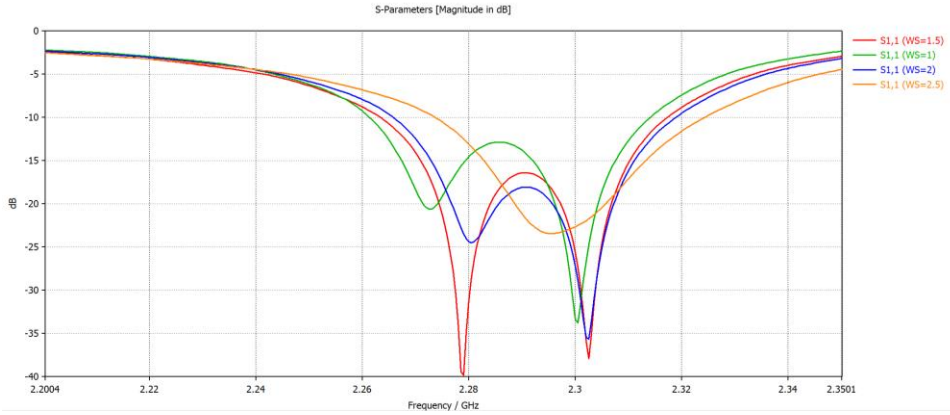

Figure 3.14: Reflection coefficients for different values of W_s.

For validation of the final structure with full-wave electromagnetic simulation, the optimal parameters of $L_p = 41.1\ mm$, $W_p = 44.55\ mm$, $L_f = 12\ mm$, $L_a = 33\ mm$ and $L_b = 14\ mm$ are selected, with a T-junction of the dimensions of $d_p = 62\ mm$ and width of $1.5\ mm$ and a center frequency of $f_0 = 2.27\ Ghz$ within the frequency tuning range is chosen to validate the antenna performance. The simulation result demonstrates a reflection coefficient for a combination of the variation of two capacitors values. Figure 3.15 shows the reflection coefficient of the antenna array at f_0.

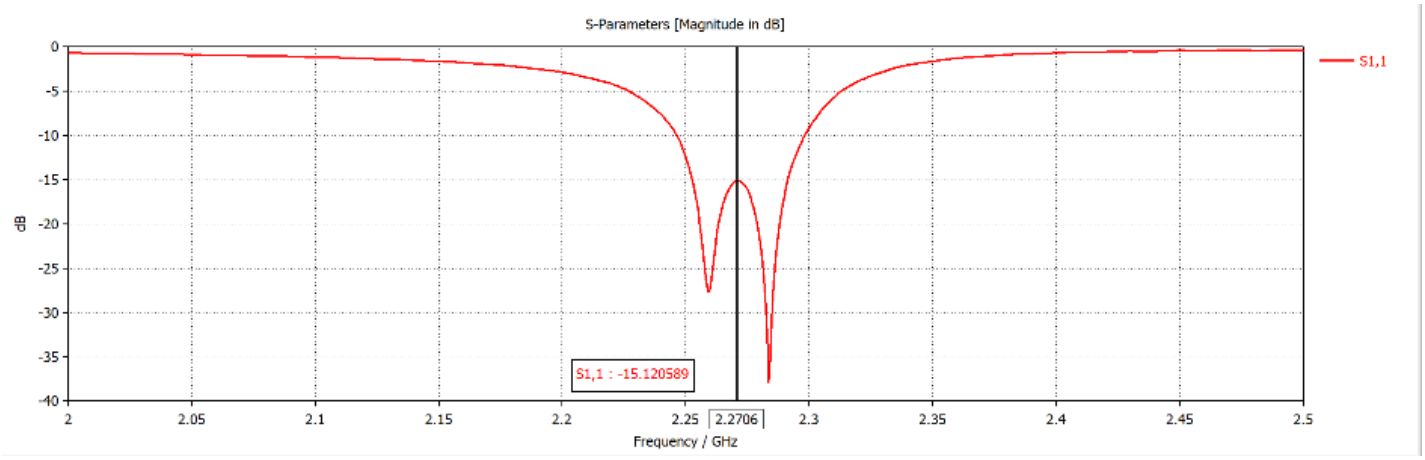

Figure 3.15: The reflection coefficient of the antenna array at $f_0 = 2.27\ GHz$.

3.3.4 The full-wave simulation for 2.27 GHz

Figure 3.16 shows the far-field radiations for three selected frequencies where the two-elements are tuned. As described in the Section 3.3.2, when the two-elements antennas have the same value of capacitor C_0, they will radiate in phase, and when either of the capacitors is slightly configured with $\pm\Delta C_0$ then it acontinuously beam-steering capability can be obtained.

Where:

(a): Same value of capacitor C_0 corresponding to broadside radiation pattern. $(0.49\ pF)$.

(b) and (c): Detuned values of capacitors by $\pm\Delta C_0$, corresponding to the beam-steering cases.

Each of the patterns has oriented with an angel of the value of $\pm 20°$ towards the orientation of the bigger capacitance value.

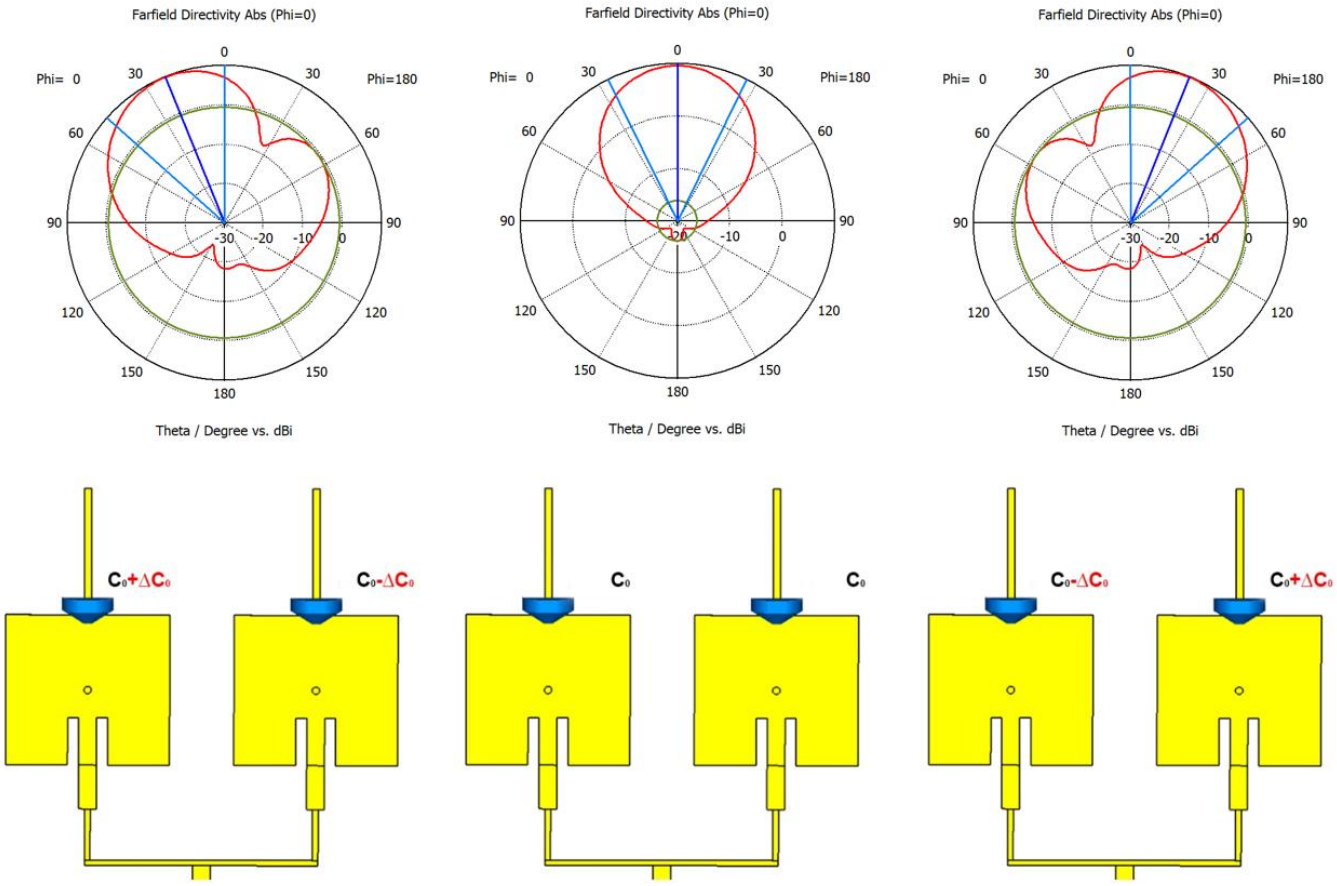

Figure 3.16: Far-field distribution at 2.27 GHz for three cases. (a): $f_1 = 2.285\ GHz$, (b): $f_0 = 2.27\ GHz$, (c): $f_2 = 2.255\ GHz$.

3.4 Reconfigurable Two-Elements Array Antenna for Ku Band

3.4.1 The Design Procedure for a Single Element Antenna Ku Band

Figure 3.17 shows the single-element antenna geometry. For this design, Rogers Duroid 5880 is selected as dielectric substrate with a relative permittivity of 2.2, loss tangent of 0.0009 and thickness of $0.508\ mm$. Using the equations mentioned in the section 3.3.1, the antenna size is chosen as $L_p = 8.05\ mm$ and $W_p = 9.775\ mm$, yielding a resonance frequency of 12 GHz.

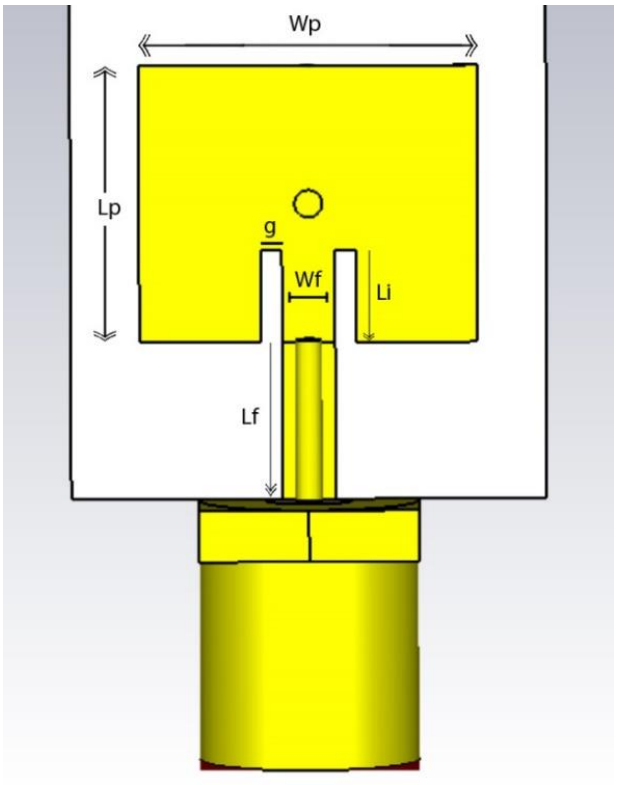

Figure 3.17: Single-element antenna for Ku band.

To introduce reconfigurability, firstly, a stub has to be added to maintain the resonance after adding a varactor diode to this patch, the stub's dimensions were picked according to its best reflection coefficient result. Some samples of the results of it while its reconfiguration are shown in the Figure 3.18 down below. The final dimensions of the stub are $W_s = 0.5\,mm$ and $L_s = 12.3\,mm$. To set the antenna as the DC ground, a shorting via is added in the center of the patch, where it does not affect the resonant patch mode.

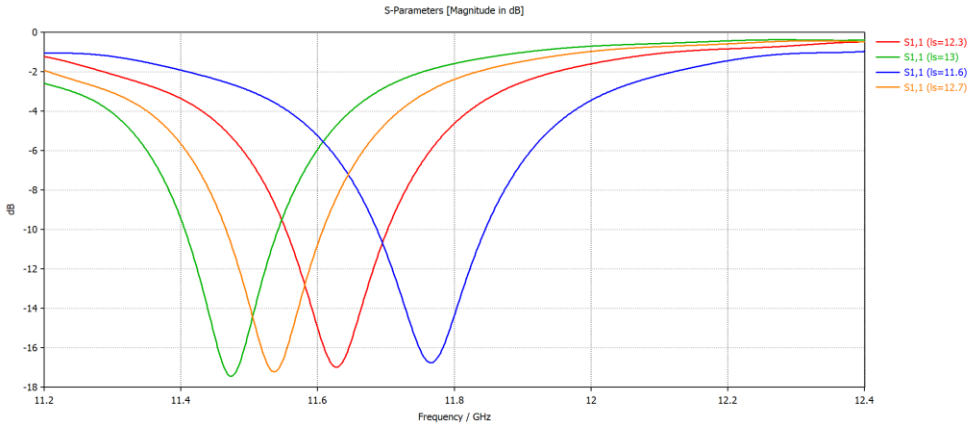

Figure 3.18: Reflection coefficients for different values of L_S.

The inset feed arrangement with line width $W_f = 1.547\,mm$, gap $g = 0.6\,mm$ and position $L_f = 4.595\,mm$ is optimized to provide impedance matching between the antenna and a 50Ω feed network. The single element antenna reconfigurable is shown in the Figure 3.19.

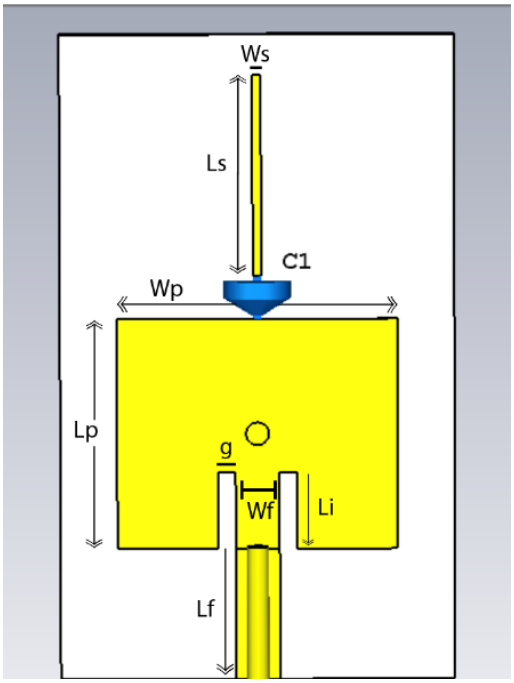

Figure 3.19: Single-element configuration for Ku band.

Figure 3.20 shows the tuning range of the single element's resonance frequency at different capacitor values ranging from 0.2 pF to 0.1 pF.

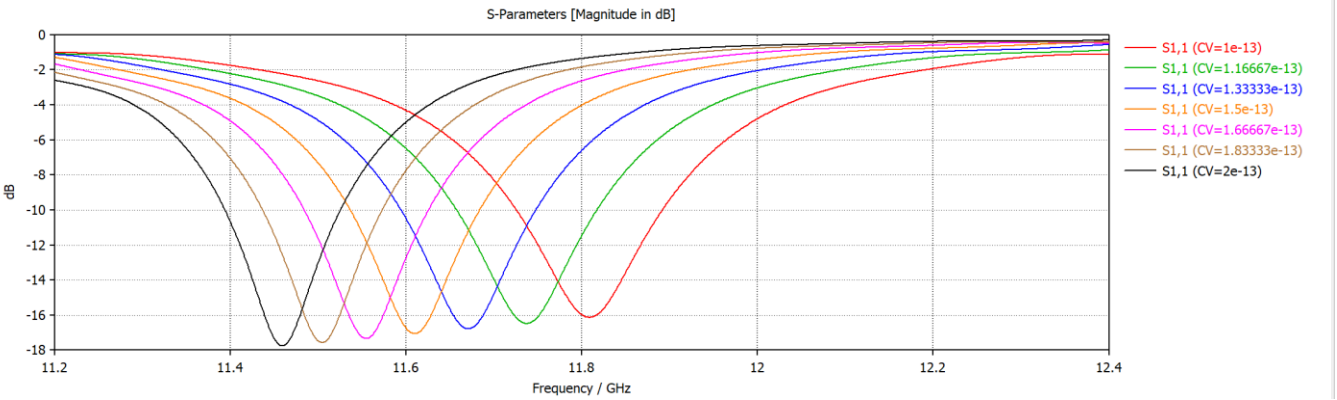

Figure 3.20: The tuning range of the resonance frequency for Ku band.

3.4.2 The Design Procedure for Two-Elements Array Antenna for Ku Band

As shown in Figure 3.21, two reconfigurable patch elements with inter-element distance $d_p = 16.2\,mm$ are fed by a T-junction power divider by the dimensions of $L_f = 2\,mm$, $L_b = 2.mm$ and $L_a = 5.2\,mm$, and a slightly different gap with $g = 0.6\,mm$ and $L_i = 2.5\,mm$. The feed network is designed with 50-Ω microstrip line, then divided up into two 100-Ω splitting in-phase feed lines. The size of the substrate is selected to $L_{sub} \times W_{sub} = 33\,mm \times 35.66\,mm$.

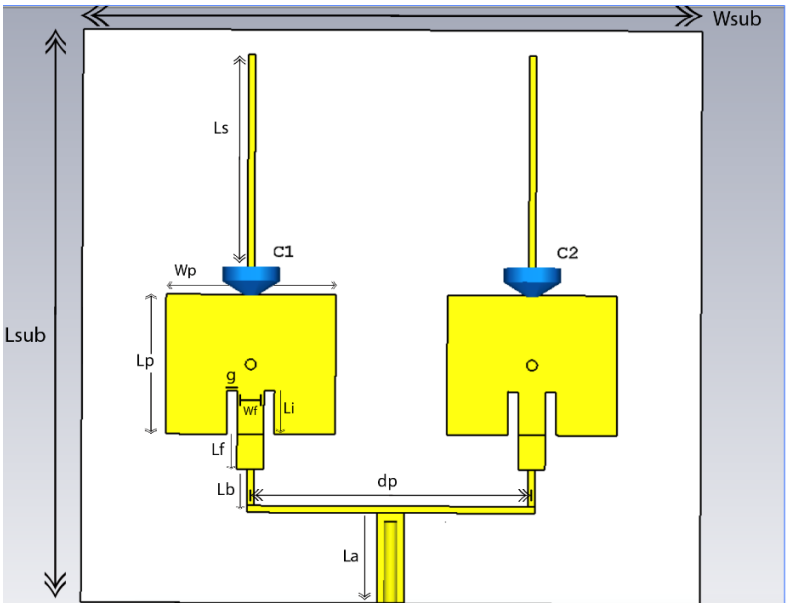

Figure 3.21: The reconfigurable two-element antenna configuration for Ku band.

The distance between the 2 antennas d_p and the width L_b have been studied. Figures 3.22 and 3.23 show the variation of S11 for the different values of d_p and L_b, respectively.

We notice that either of d_p or L_b doesn't really affect the matching impedance.

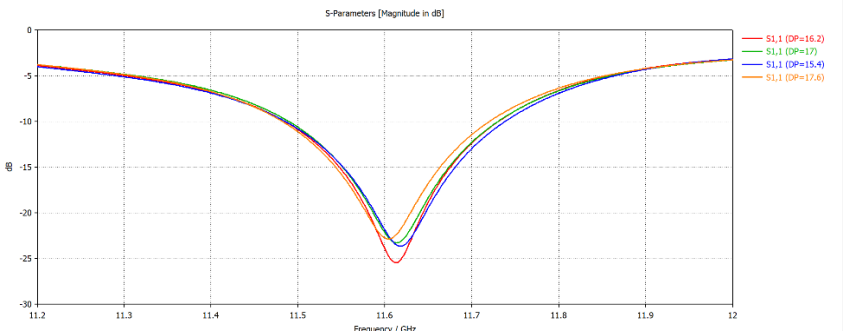

Figure 3.22: Reflection coefficients for different values of d_p.

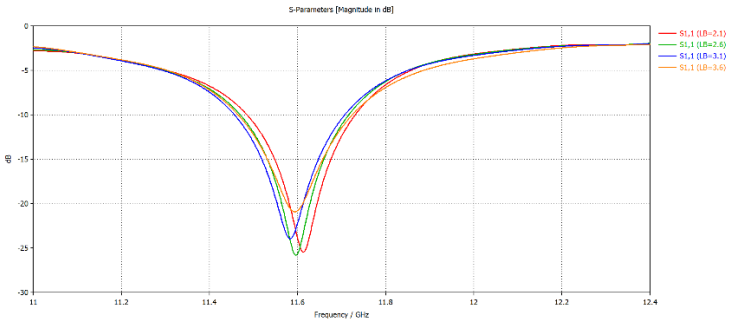

Figure 3.23: *Reflection coefficients for different values of L_b.*

3.4.3 The Dephasing Process

In this case, the phase difference between the two elements is also obtained by adjusting the effective electrical length of the individual patches through variation of the varactor capacitance. As a starting point, a particular resonance frequency $f_0 = 11.635\ GHz$ can be tuned by adjusting the varactor capacitance $C_0 = 0.145\ pF$. Then, if a slight capacitance variation $\pm\Delta C_0 = 0.02\ pF$ is introduced for the two elements (one positive, one negative), selected by the actual bandwidth of the accepted f_0 values, (starting from -10 dB), the patches become slightly detuned from their resonance. Figure 3.24 shows this actual example graphically.

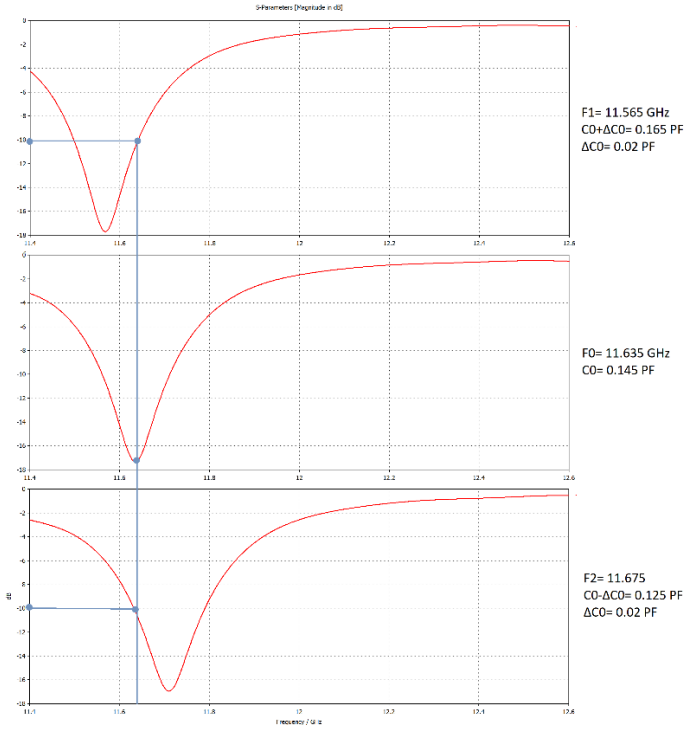

Figure 3.24: *Detuning of the patch from resonance frequency for Ku band.*

The Figure 3.25 shows the current distribution on the patch for the 3 cases. We observe that, for the 3 frequencies: $f_0 = 11.635\ GHz$, $f_1 = 11.565\ GHz$, $f_2 = 11.675\ GHz$, currents are spread out over the patch which prove operation at these 3 frequencies.

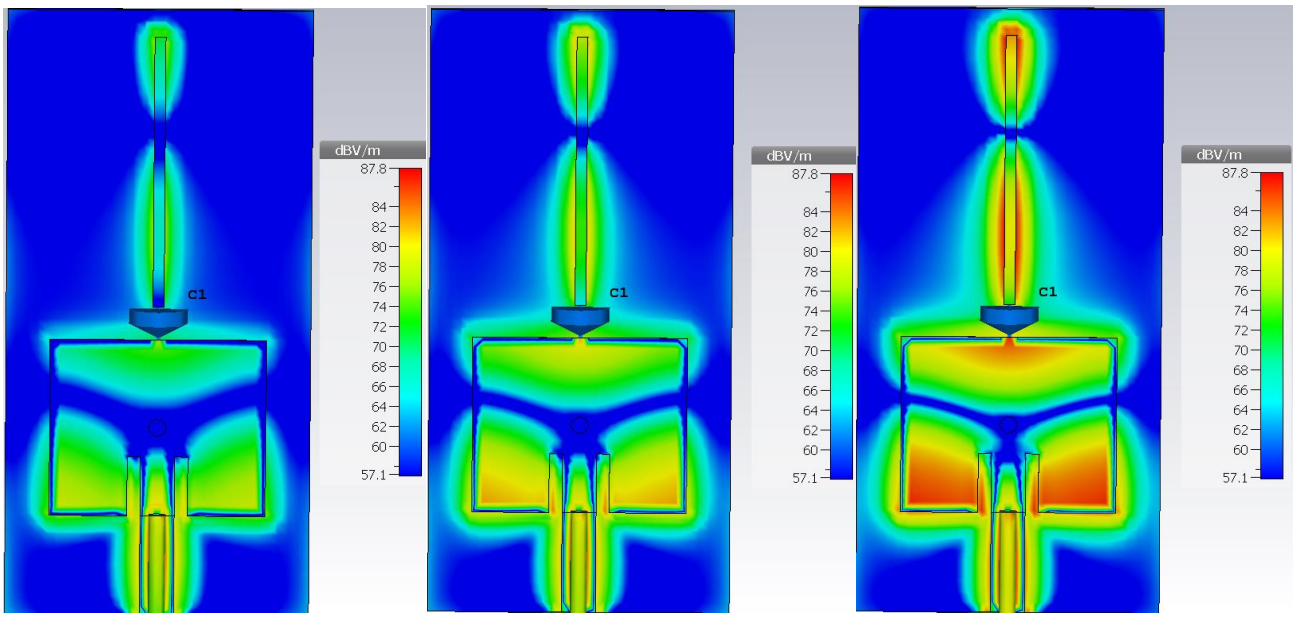

(a) (b) (c)

Figure 3.25: The current distribution on the patch for the 3 cases; (a): $f_1 = 11.565\ GHz$, (b): $f_0 = 11.635\ GHz$, (c): $f_2 = 11.675\ GHz$.

3.4.4 The Full Wave Simulations for Ku band

For validation of the final structure with full-wave electromagnetic simulation, the optimal parameters of $L_p = 8.05\ mm$, $W_p = 9.775\ mm$, $L_f = 2\ mm$, $L_a = 5.2\ mm$ and $L_b = 2.1\ mm$ are selected, and a center frequency of $f_0 = 11.635\ Ghz$ within the frequency tuning range is chosen to validate the antenna performance. The simulation result demonstrates a reflection coefficient for a combination of the two capacitors values fixed both at $C_0 = 0.145\ pF$.

Figure 3.26 shows the reflection coefficient of the antenna array at f_0.

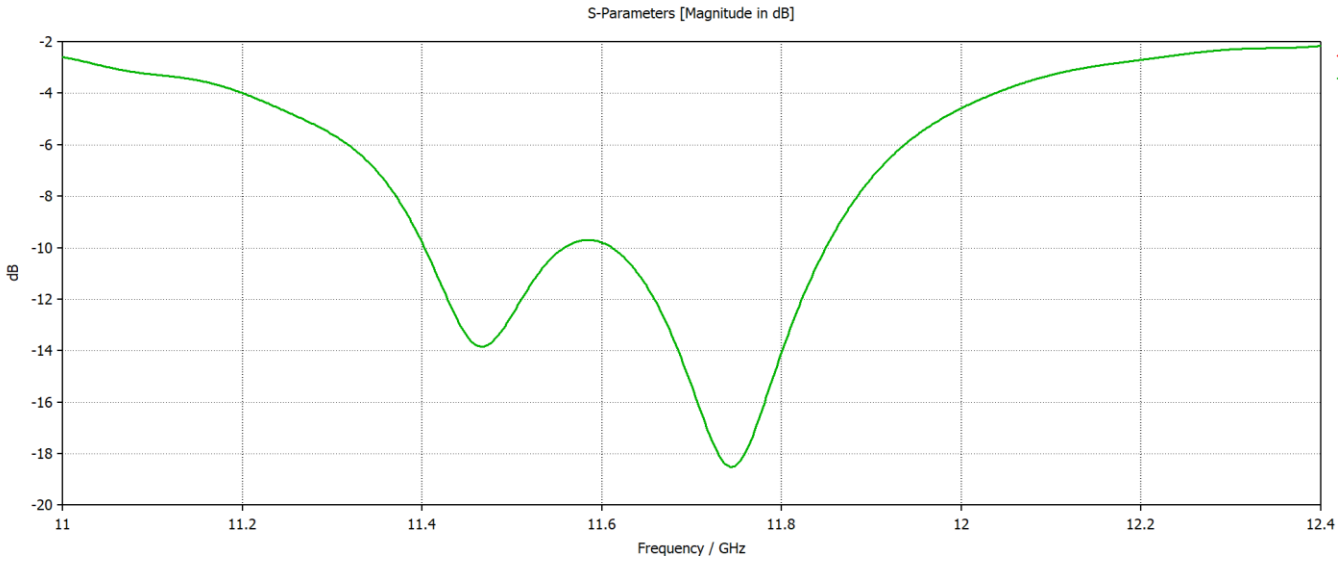

Figure 3.26: *The reflection coefficient of the antenna array at f_0.*

Figure 3.27 shows the far-field distributions, as well as the voltage distributions for three selected scenarios where the two-elements are tuned at or near the resonant frequency of 11.635 GHz. As described in the Section 3.3.2, when the two-elements antennas have the same value of capacitor C_0, they will radiate in phase, and when either of the capacitors is slightly configured with $\pm\Delta C_0$ then it a continuously beam-steering capability can be obtained.

Where $C = C_0 \pm \Delta C_0$; $C_0 = 0.145\ pF$ and $\Delta C_0 = 0.02\ pF$.

First graph is for the same value of capacitor C_0 corresponding to broadside radiation pattern. $(0.145\ pF)$. Where the current is equally distributed on both patches.

(b) and (c): Detuned values of capacitors by $\pm\Delta C_0$, corresponding to the beam-steering cases. Each of the patterns has oriented with an angel of the value of $\pm 20°$ towards the orientation of the bigger capacitance value, and each current distribution is related to the bigger value of the capacitance C_0 on one patch compared to its value on the other patch.

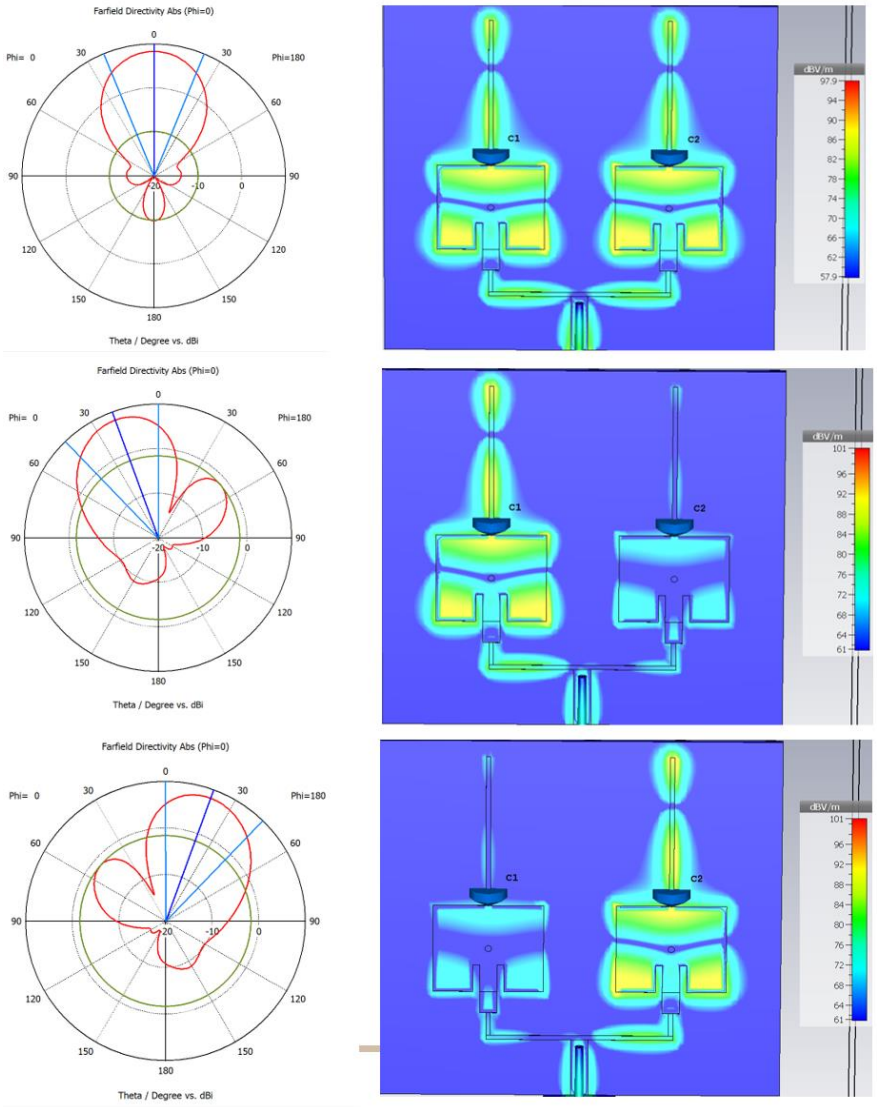

Figure 3.27: Far-field distribution for three cases; (a): $f_1 = 11.565\ GHz$, (b): $f_0 = 11.635\ GHz$, (c): $f_2 = 11.675\ GHz$.

3.5 Conclusion

In this chapter, a single-element antenna has been designed and adapted to be reconfigurable with a variation in the varactor value.

A two-element array antenna with frequency and pattern reconfigurability has also been proposed. A tuning mechanism based on stub-loaded varactors has been adopted to realize a phase shift between two slightly detuned antenna elements. Based on this principle, the antenna has been parametrically optimized to reach a continuous beam scanning across a relative frequency tuning range in 11.635 GHz.

Conclusion and Perspectives

This thesis has been inspired by the concept of stub-loaded varactor control for the study and development of novel reconfigurable antenna designs. Various configurations have been proposed across numerous generic communications applications, with agility of the antennas demonstrated in terms of multiple operating frequencies and radiation patterns.

Chapter 1 has given general introduction about Microstrip antennas and some basic information when it comes to the telecommunication and radio engineering field, it introduces also the main elements to obtain a radio communication as well as a definition of radiation parents and other antennas characteristic such as gain, efficiency, bandwidth and directivity.

On the other hand, Chapter 2 introduced the reconfigurable antenna technology and explained the different reconfiguration mechanisms as well as a general introduction about radiation pattern-reconfigurable antennas. In addition to that, in this chapter we explained the existence of the reconfigurability of antennas in Ku-band and its different applications.

Chapter 3 has been identified as the first major contribution part of this thesis. This chapter focused on electronically reconfigurable beam steering antennas, able to operate within a tunable frequency band. The operating frequency and phase control have been achieved by using capacitances together with additional loading from open circuit stubs. The achievement of a continuously beam-steerable radiation pattern has been presented in detail in this chapter.

For the purpose of beam scanning, a reconfigurable two-element patch array antenna has been presented in Chapter 3. A capacitance has been used as a tuning mechanism in order to selectively modify the characteristics of the electrical length or current distribution of each antenna element. In the antenna design procedure, a rectangular single-element patch has been first considered with a capacitance placed at the edge of the antenna open aperture to obtain reconfigurability. This results in a wide frequency tuning range with enhanced performance achieved through stub parameter optimization. As mentioned in this chapter, the capacitance C_0 was controlled to variate from 1.305 pF to 0.149 pF in the 2.27 GHz manipulation, and from 0.125 pF to 0.165 pF in the Ku-band manipulation.

In this reconfigurable design, a relative phase shift which can be exploited for beam scanning also can be determined for each single element when detuned around its resonance. To achieve

beam scanning at a given frequency, firstly, an operating frequency f_0 is identified by adjusting the varactor capacitance C_0. Then, by introducing a small additional capacitance ΔC_0 with opposite signs around C_0, both patches are slightly detuned from their resonance. As a result, a phase shift is introduced between the two element antennas which allow beam scanning functionality. The two reconfigurable patch elements are placed next to each other in an array configuration with an inter-element distance d_p and they are fed by a T-junction power divider. In this configuration, the optimization of the mutual coupling effects between the elements and through the feeding line must be taken into account to achieve a maximum beam scanning angle for the antenna. To gain a better understanding of the operation principle, the antenna can be operated in various states at a given frequency f_0. When the two elements share the same capacitance value of C_0, they radiate in phase resulting in a broadside radiation pattern. Meanwhile, when the two elements are detuned through respective addition of the ΔC_0, a continuous H-plane beam scanning ranging from -20° to +20° around broadside can be obtained. The antenna thus demonstrates multiple functionalities since it is frequency and pattern reconfigurable.

Finally, as a general conclusion, the potential of the uses in the Ku band would be significantly important if properly exploited, this thesis has described the ability of designing and implementing reconfigurable antennas based on varactor-loaded stubs in the Ku band, within the frequency of $f_0 = 11.635\ GHz$ precisely, which demonstrates the capability of the approach to apply such technology for satellite applications.

The perspective of this work is to realize the proposed structure, measured it and validates the simulation results.

Bibliography

[1] R. L. Haupt and M. Lanagan, “Reconfigurable antennas,” IEEE Antennas Propag. Mag., vol. 55, no. 1, pp. 49–61, 2013, doi: 10.1109/MAP.2013.6474484.

[2] P. Qin, Y. J. Guo, S. Member, Y. Cai, and E. Dutkiewicz, “A Reconfigurable Antenna With Frequency and Polarization Agility,” vol. 10, pp. 1373–1376, 2011.

[3] S. Onat, M. Ünlü, L. Alatan, Ş. Demir, and T. Akin, “Design of a Re-configurable dual frequency microstrip antenna with integrated RF MEMS switches,” IEEE Antennas Propag. Soc. AP-S Int. Symp., vol. 2 A, pp. 384–387, 2005, doi: 10.1109/APS.2005.155182".

[4] H. Steyskal, R. A. Shore, and R. L. Haupt, “Methods for Null Control and Their Effects on the Radiation Pattern.,” IEEE Trans. Antennas Propag., vol. AP-34, no. 3, pp. 404–409, 1986, doi: 10.1109/tap.1986.1143816.

[5] BALANIS-C. A. (2015). Antenna Theory: Analysis and Design, Hoboken: "John Wiley and Sons, Incorporated".

[6] Balanis, Antenna Theory: "Analysis and Design, April 1982.".

[7] Institute of Electrical and Electronics Engineers, “The IEEE standard dictionary of electrical and electronics terms”; 6th ed. New York, N.Y., Institute of Electrical and Electronics Engineers, c1997. IEEE Std 100-1996.

[8] REBEIZ-G., TAN-G.-L., AND HAYDEN-J. (2002). "RF MEMS phase shifters: design and applications", IEEE Microwave Magazine, 3(2), pp. 72–81.

[9] HUM-S. V., OKONIEWSKI-M., AND DAVIES-R. J. (2005b)." Realizing an electronically tunable reflect array using varactor diode-tuned elements", IEEE Microwave and Wireless Components Letters, 15(6), pp. 422–424.

[10] XIAO-S., ZHENG-C., LI-M., XIONG-J., AND WANG-B.-Z. (2015b). "Varactor-loaded pattern reconfigurable array for wide-angle scanning with low gain fluctuation", IEEE Transactions on Antennas and Propagation, 63(5), pp. 2364–2369

[11] Jonsson, Magnus & Vinel, Alexey & Bellalta, Boris & Tirkkonen, Olav. (2015). Multiple Access Communications: 8th International Workshop, MACOM 2015, Helsinki, Finland, September 3-4, 2015, Proceedings. 10.1007/978-3-319-23440-3.".

[12] A. Zohur, H. Mopidevi, D. Rodrigo, M. Unlu, L. Jofre, and B. A. Cetiner, “RF MEMS reconfigurable two-band antenna,” IEEE Antennas Wirel. Propag. Lett., vol. 12, no. Mode 1, pp. 72–75, 2013, doi: 10.1109/LAWP.2013.2238882.

[13] PATEL-S. K., ARGYROPOULOS-C., AND KOSTA-Y. P. (2018). "Pattern controlled and frequency tunable microstrip antenna loaded with multiple split ring resonators", IET Microwaves, Antennas and Propagation, 12(3), pp. 390–394

[14] OUYANG-J., PAN-Y. M., AND ZHENG-S. Y. (2018). "Center-fed unilateral and pattern reconfigurable planar antennas with slotted ground plane", IEEE Transactions on Antennas and Propagation, 66(10), pp. 5139–5149.

[15] BORHANI-M., REZAEI-P., AND VALIZADE-A. (2016). Design of a reconfigurable miniaturized microstrip antenna for switchable multiband systems, IEEE Antennas and Wireless Propagation Letters, 15, pp. 822 – 825.

[16] ZAINARRY-S. N. M., NGUYEN-TRONG-N., AND FUMEAUX-C. (2018). "A frequency and pattern-reconfigurable two-element array antenna", IEEE Antennas and Wireless Propagation Letters, 17(4), pp. 617–620

[17] ROW-J.-S., LIU-W.-L., AND CHEN-T.-R. (2012). "Circular polarization and polarization reconfigurable designs for annular slot antennas", IEEE Transactions on Antennas and Propagation, 60(12), pp. 5998–6002.

[18] S. Zhang, "A Pattern Reconfigurable Microstrip Parasitic Array: Theory, Design and Applications," University of Illinois at Urbana–Champaign, 2005.

[19] J. T. Bernhard, "Reconfigurable antennas", vol. 4. 2007.

[20] A. M. Abdin, “12 GHz planar array antenna for satellite communication,” Prog. Electromagn. Res. Symp., vol. 1, pp. 208–211, 2008, doi: 10.2529/piers071003071500.

[21] J. D. Zhang, W. Wu, and D. G. Fang, “Dual-band and dual-circularly polarized shared-aperture array antennas with single-layer substrate,” IEEE Trans. Antennas Propag., vol. 64, no. 1, pp. 109–116, 2016, doi: 10.1109/TAP.2015.2501847.

[22] S. Perhirin and Y. Auffret, “A low consumption electronic system developed for a 10km long all-optical extension dedicated to sea floor observatories using power-over-fiber technology and SPI protocol.,” Microw. Opt. Technol. Lett., vol. 55, no. 11, p".

[23] K. A. Solanki, “Study and Analysis of Microstrip Patch Array at 12 GHz for 5G Applications,” vol. 4, no. 1, pp. 1–8, 2018.

[24] CST, "https://www.3ds.com/products-services/simulia/products/cst-studio-suite/".

[25] JUSOH-M., SABAPATHY-T., JAMLOS-M. F., AND KAMARUDIN-M. R. (2014b). "Reconfigurable four-parasitic-elements patch antenna for high-gain beam switching application", IEEE Antennas and Wireless Propagation Letters, 13, pp. 79–82.